Cosmic Rays (CR), Atmospheric Muons and Simulation Techniques

Germano Bonomi
University of Brescia
INFN Pavia

Summary

o) Primary cosmic rays
o) Secondary cosmic rays
o) Muons at the ground
o) A muon Monte Carlo simulation
o) Muon generators

An example

The fantastic 4: N. 1 (1961)

The first “space” expeditions

CR history in one slide

- Cosmic radiation (CR) is known since the beginning of the 20th century

  - experiments by Wulf, Pacini and Hesse (1912) led to hypothesize the existence of a cosmic radiation

- Since its discovery, cosmic radiation allowed several discoveries in fundamental physics:

  - positron (1932), muon (1937), pion (1947), kaon (1947), Λ (1951), …

- Even today, in the “accelerator era”, CR are still widely studied

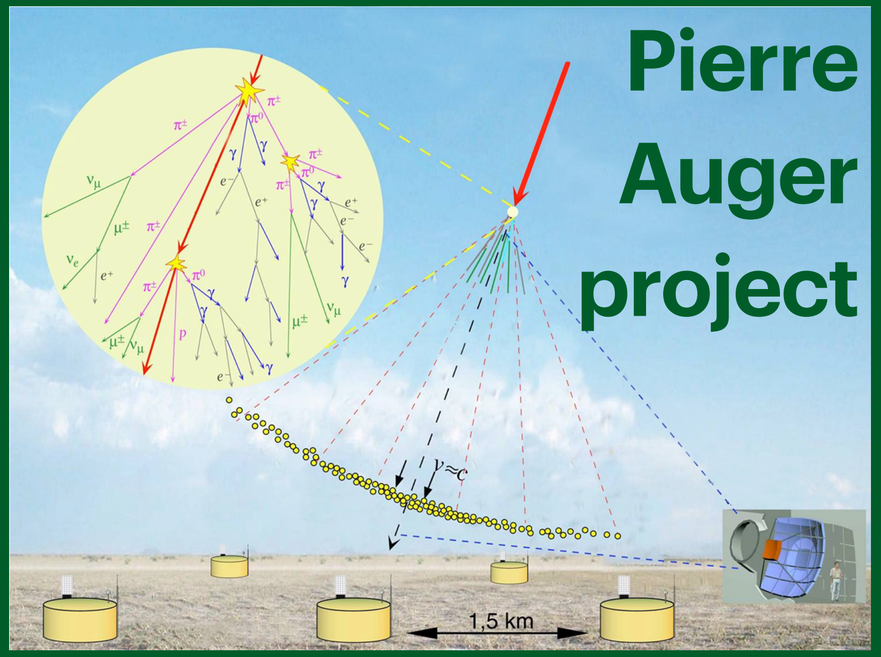

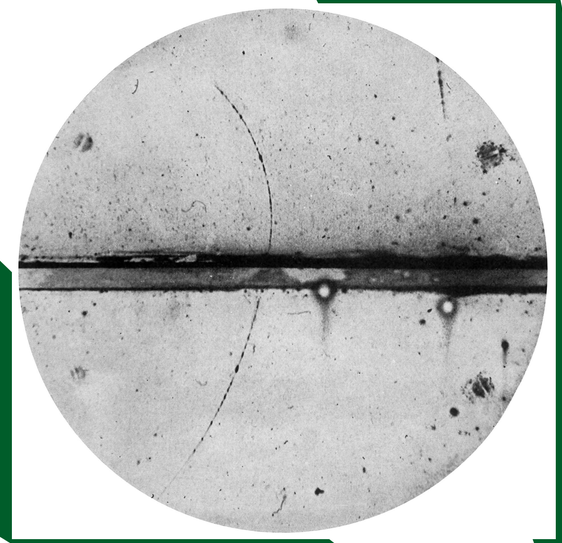

Positron discover

In 1925, as a consequence of his experiments, Millikan concluded that there was no extraterrestrial radiation…
…but changed his mind in 1926 (after further experimentation)

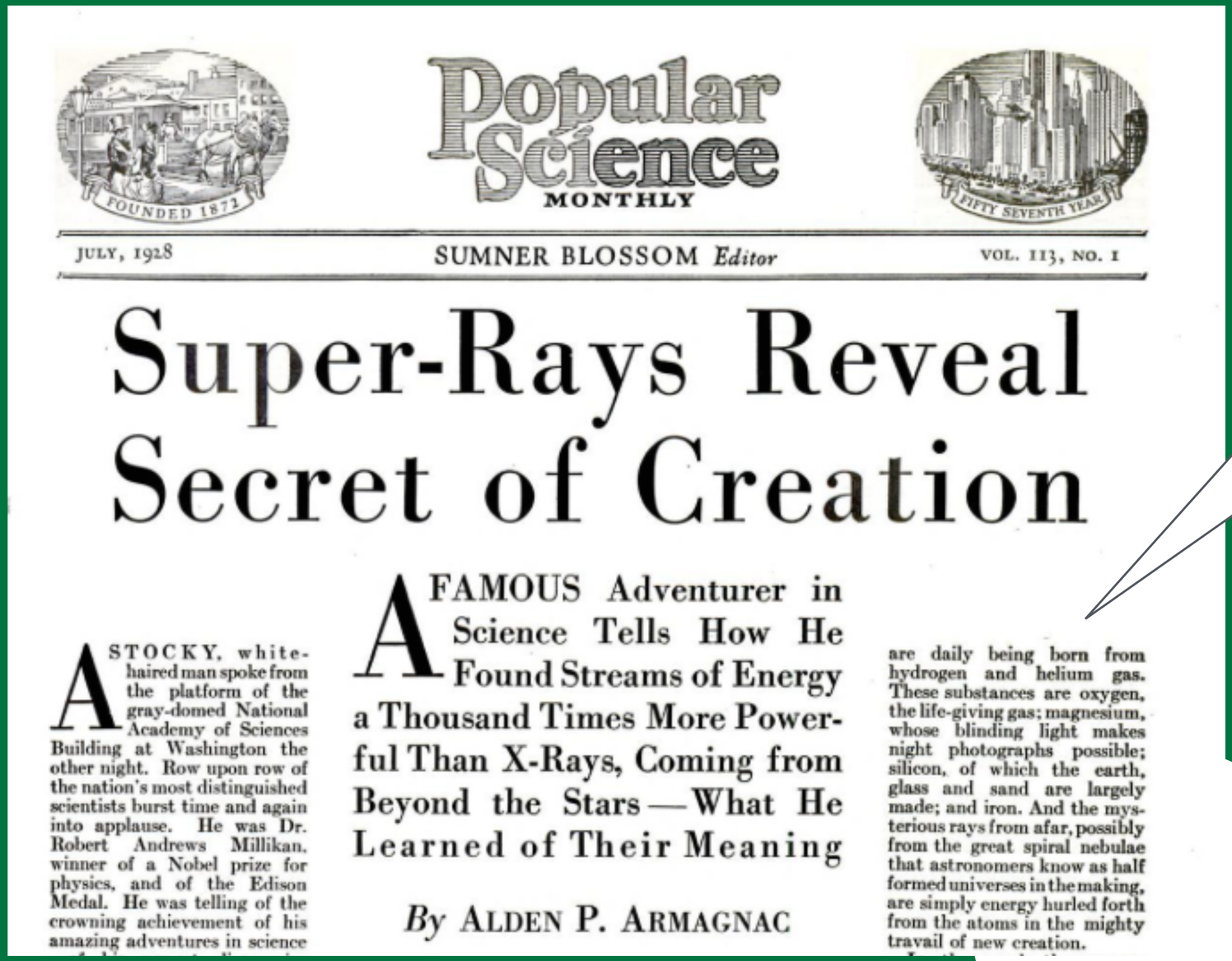

Popular Science MONTHLY

JULY, 1928 SUMNER BLOSSOM *Editor* VOL. 113, NO. 1

Super-Rays Reveal Secret of Creation

A FAMOUS Adventurer in Science Tells How He Found Streams of Energy a Thousand Times More Powerful Than X-Rays, Coming from Beyond the Stars—What He Learned of Their Meaning

By ALDEN P. ARMAGNAC

A STOCKY, white-haired man spoke from the platform of the gray-domed National Academy of Sciences Building at Washington the other night. Row upon row of the nation's most distinguished scientists burst time and again into applause. He was Dr. Robert Andrews Millikan, winner of a Nobel prize for physics, and of the Edison Medal. He was telling of the crowning achievement of his amazing adventures in science

are daily being born from hydrogen and helium gas. These substances are oxygen, the life-giving gas; magnesium, whose blinding light makes night photographs possible; silicon, of which the earth, glass and sand are largely made; and iron. And the mysterious rays from afar, possibly from the great spiral nebulae that astronomers know as half formed universes in the making, are simply energy hurled forth from the atoms in the mighty travail of new creation.

triumph. He told of struggles up rugged mountains on two continents to find and measure the elusive rays—then of a flash of inspiration only a few weeks ago that proved the rays the actual messengers of creation.

Cosmic rays to study the mysteries of the Universe

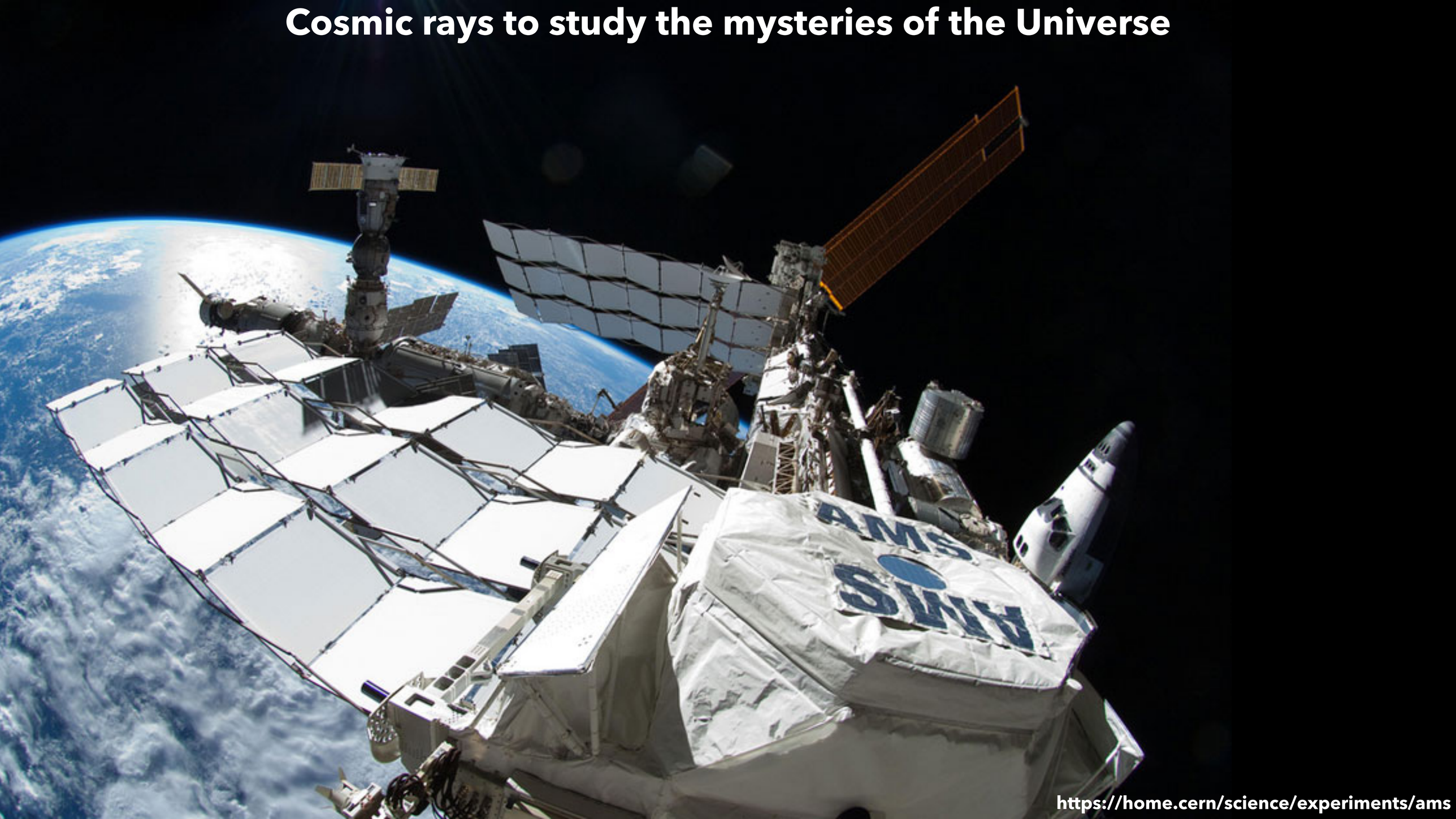

https://home.cern/science/experiments/ams

PDG particle data group
ARCHIVED EDITION

SHORTCUTS CITATION

The Review of Particle Physics (2024)

S. Navas *et al.* (Particle Data Group), Phys. Rev. D 110, 030001 (2024)

Summary Tables | Topical Index
Reviews, Tables, Plots | Downloads & API
Particle Listings
Errata

Results provided by Google

Astrophysics and Cosmology

30. Cosmic Rays

Revised March 2024 by J. Alvarez-Muñiz (Santiago de Compostela U.), Z. Cao (IHEP Beijing), U.F. Katz (Erlangen U.), P. Mertsch (TTK, RWTH) and C. Spiering (DESY, Zeuthen).

30.1 Theory

Cosmic rays (CRs) are a non-thermal population of particles that pervade the Universe. Their salient characteristics can be inferred from their major observational properties: spectrum, composition and arrival directions. For charged CRs, the energies extend from tens of MeV to close to 1 ZeV, the intensity is $\sim 10^4\,\mathrm{m}^{-2}\,\mathrm{s}^{-1}\,\mathrm{sr}^{-1}$ above 1 GeV, but the differential spectrum falls steeply with energy E, following a power-law dependence $E^{-\gamma}$. The most striking spectral features are the "knee" at a few PeV where the spectral index γ changes from ~ 2.7 to ~ 3, the "second knee" at ~ 100 PeV with a change to ~ 3.3 and the "ankle" at a few EeV where γ changes to ~ 2.5. The flux is largely suppressed above a few tens of EeV. (More detailed discussion of spectral features can be found below in Secs. 30.2.1 and 30.2.2.) Charged CRs are composed mostly of protons, helium, and other nuclei, as well as electrons, positrons and anti-protons. The arrival directions are mostly isotropic, but below and around the knee interesting $\mathcal{O}(10^{-4}\ldots10^{-3})$ anisotropies due to the distribution of sources and properties of the Galactic magnetic fields have been observed, reaching $\sim \mathcal{O}(10^{-1})$ at the highest energies. Gamma-rays can be resolved into those from astrophysical sources ($\sim$ 6660 [1] above 50 MeV, $\sim$ 300 [2, 3] at TeV energies), plus diffuse fluxes of galactic and extra-galactic origin, predominantly showing power-law dependence on energy. The observation of high-energy neutrinos has opened a new window; while the distribution is largely isotropic, evidence for two extra-galactic sources as well as for a contribution from the galactic plane has been found. The energy spectra of charged CRs, diffuse gamma-rays and neutrinos are shown in Fig. 30.1. Combined observations of charged CRs, gamma-rays and neutrinos as well as gravitational waves (see Sec. 21.2.3) allow for valuable insights into the most extreme astrophysical environments and is referred to as multi-messenger astrophysics. Adding the contribution from all species results in the all-particle spectrum. While it was believed for a long-time that it was a featureless power law up to the knee at a few PeV, it has now been recognized that it has much more structure, mirroring the features in the individual species. These features carry important information on the acceleration and transport of CRs.

99% of the primary
cosmic rays
are from outer space
(1% Sun)

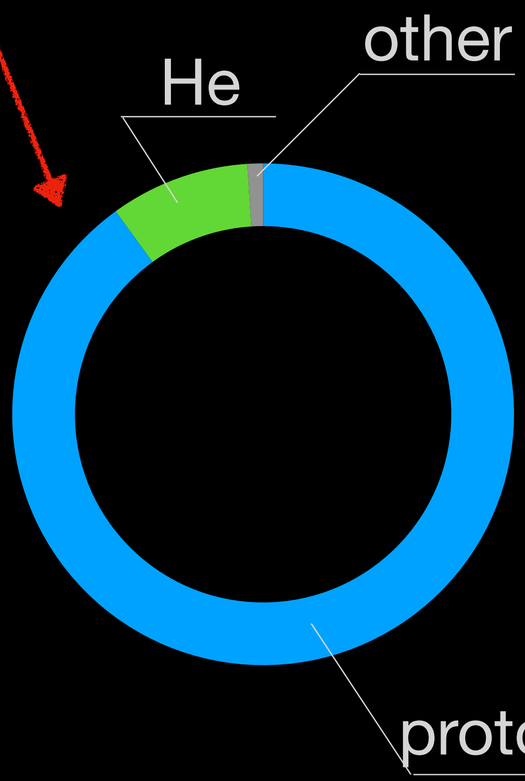

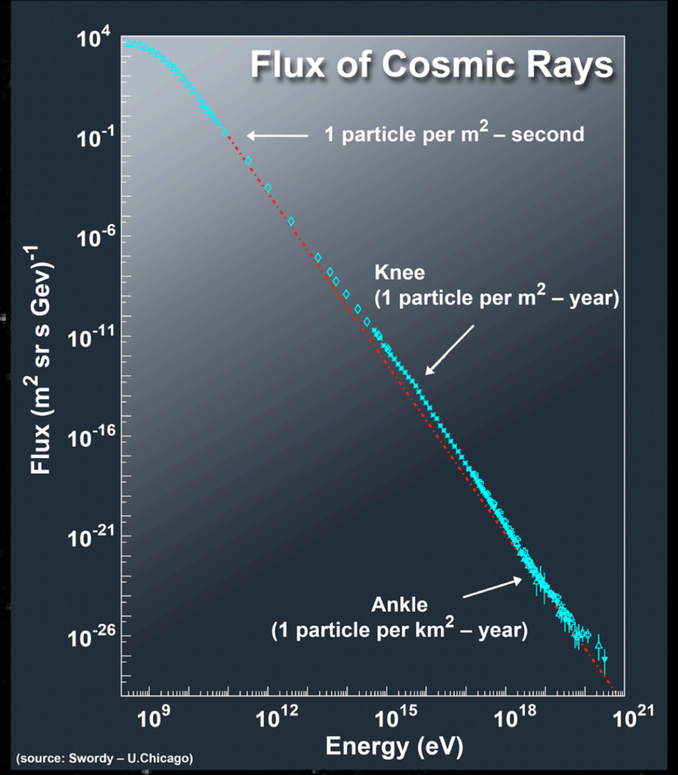

Photon
Neutrino
Charged cosmic ray
(ex.: Proton)

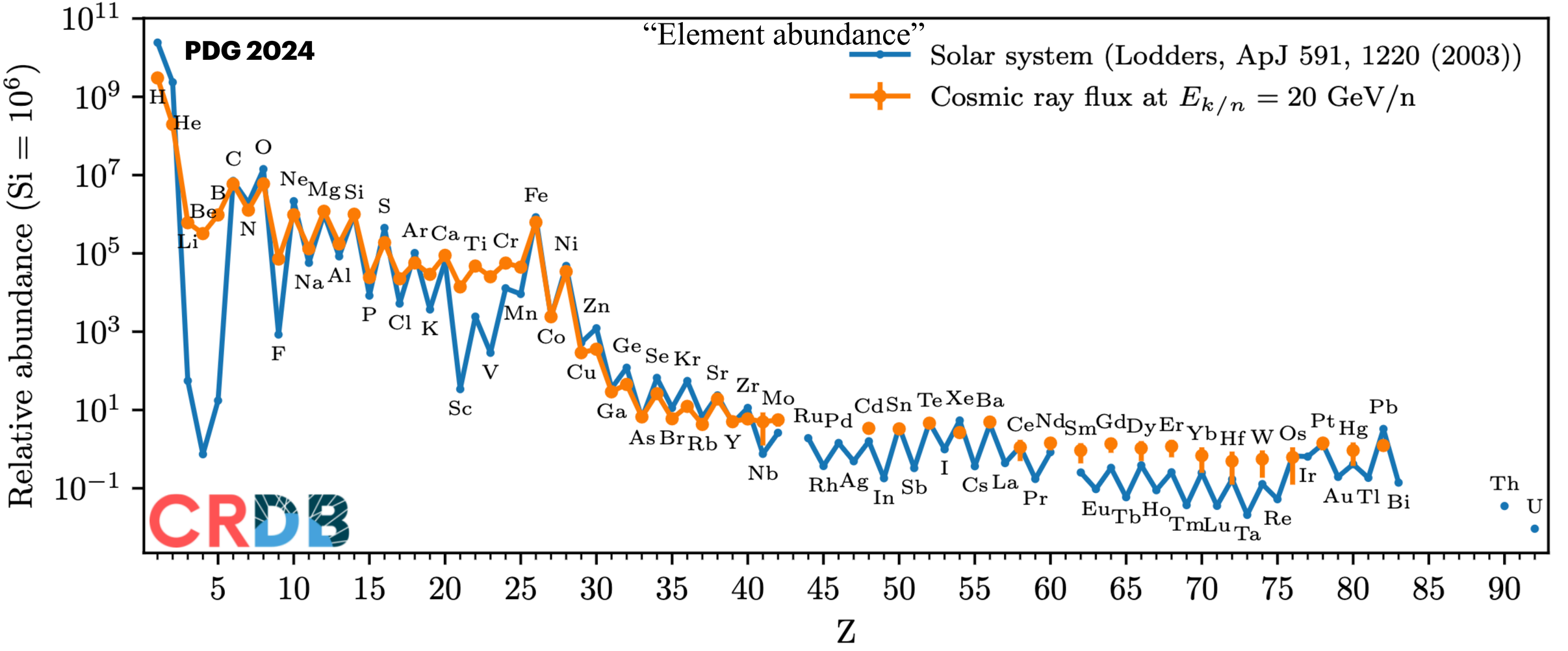

Figure 30.2: CR abundances compared with solar system ones [58]. Modified from [35].

Charged CRs are deflected by magnetic fields and so generally speaking the observed events do not point back to sources.

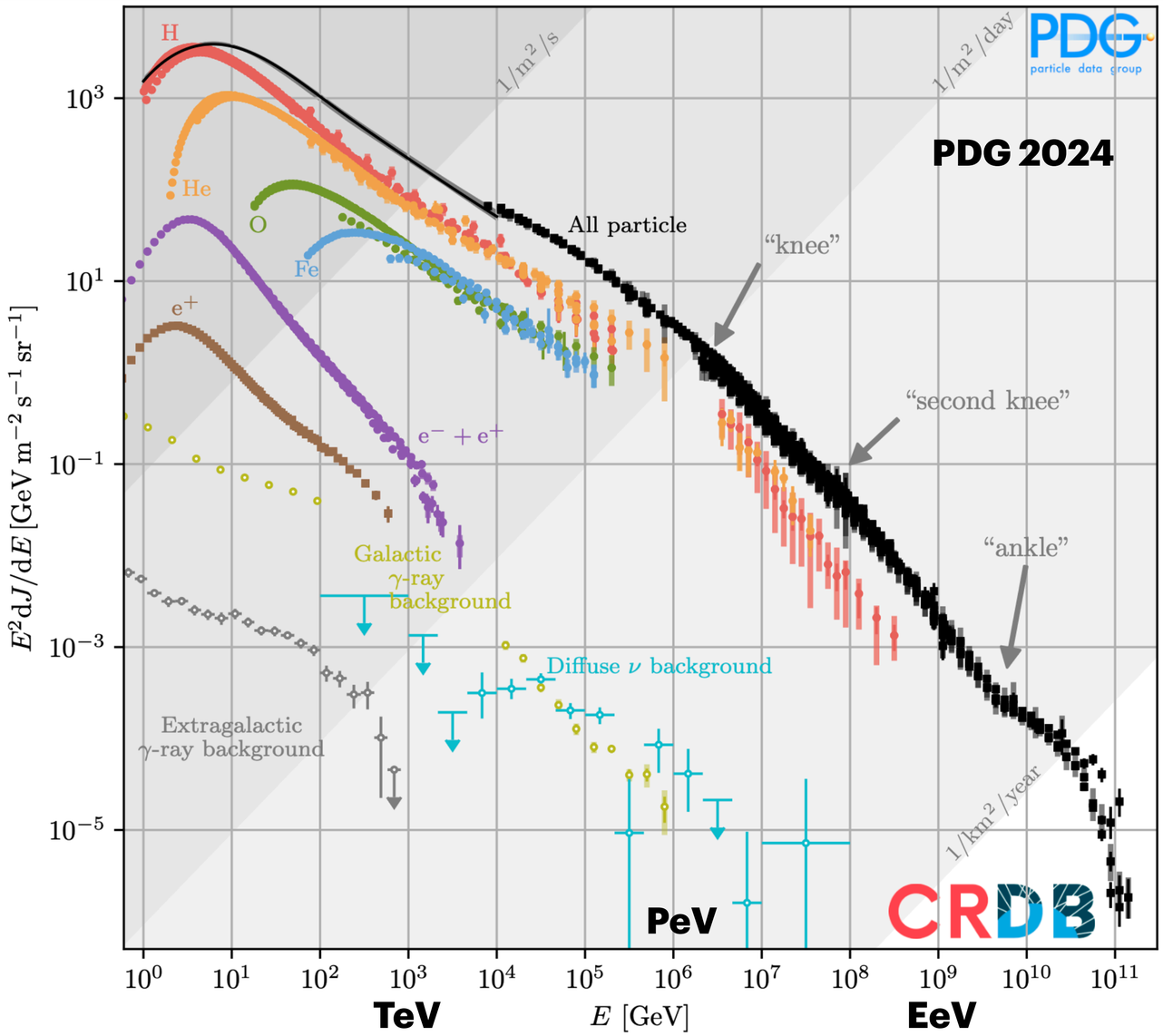

Figure 30.1: The spectrum of cosmic rays (CRs). Shown are measurements of the intensity of charged and neutral CRs, multiplied by kinetic energy squared. The data for the charged CRs [5–34] have been extracted from the Cosmic Ray Database (CRDB) [35]. Below 10^4 GeV, the all-particle spectrum is the sum of spline fits of the most important nuclear species. The diffuse γ-ray fluxes have been extracted from Refs. [36–38], measurements of the diffuse neutrino background from Ref. [39]. Energy-integrated intensities are indicated by the various diagonal lines.

Between hundreds of MeV and at least a few PeV, CRs are believed to be of galactic origin; above a few EeV, the sources are most likely extra-galactic.

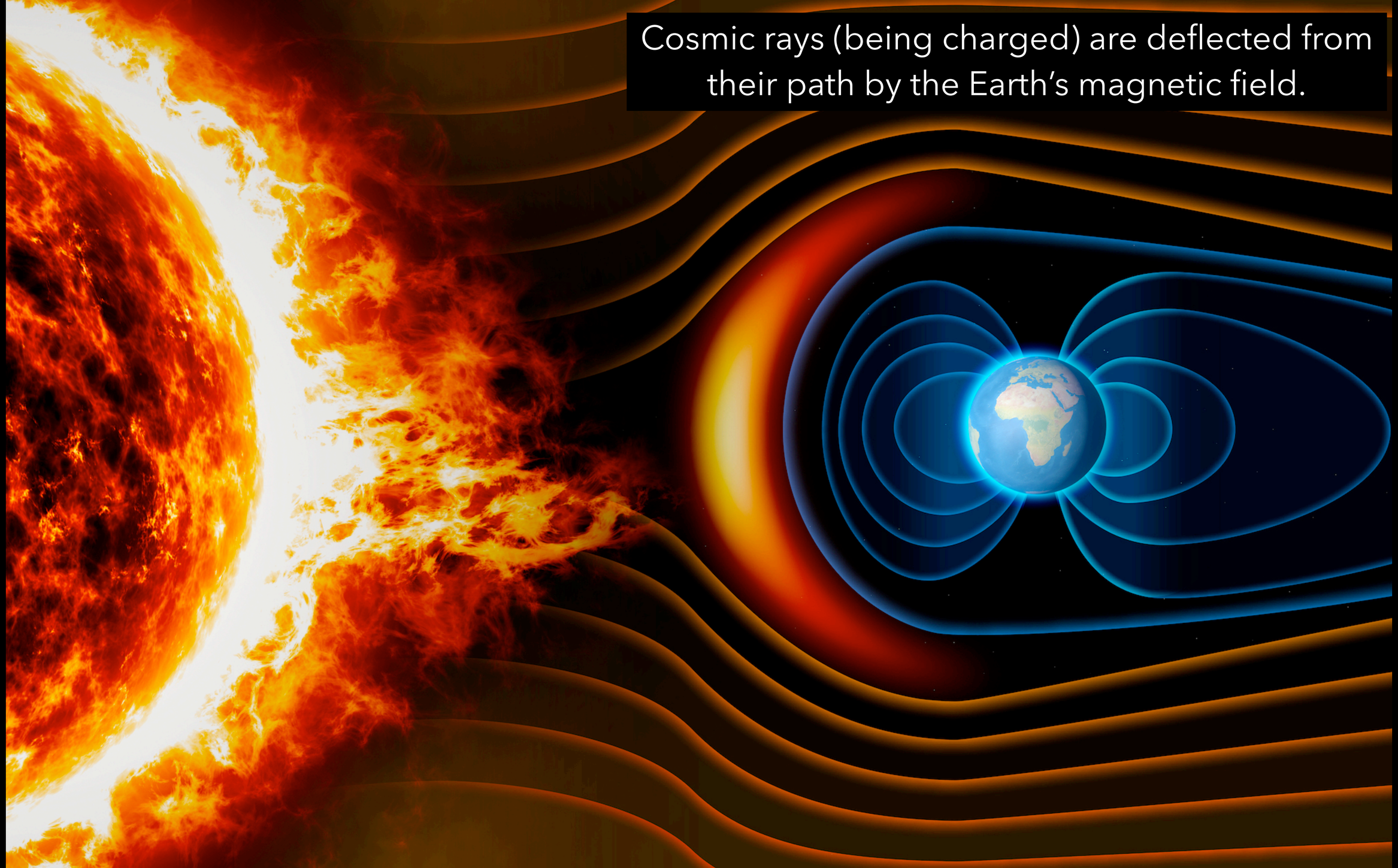
Cosmic rays (being charged) are deflected from their path by the Earth's magnetic field.

Secondary cosmic ray showers

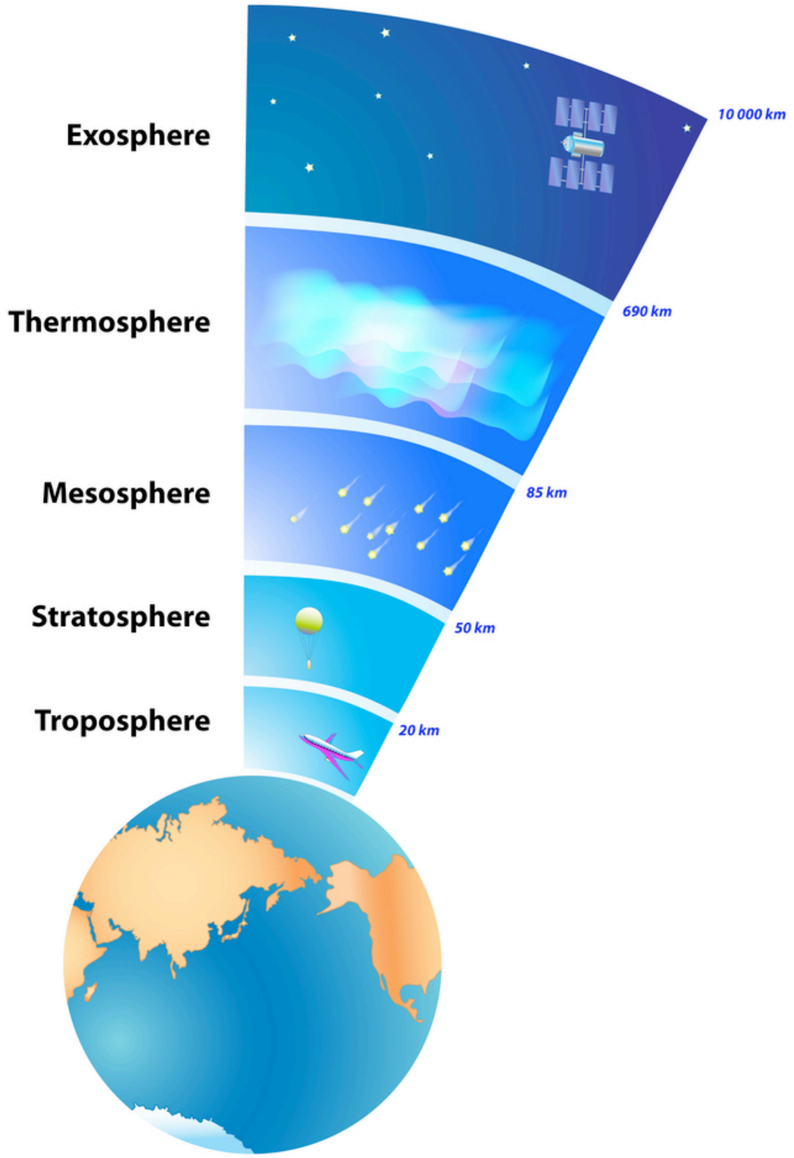

Air shower
[NASA image]

When an energetic (E ~ 1 PeV) cosmic proton or nucleus interacts with a nucleus of air, it generates between a few and hundreds of secondary particles depending on its energy. On average ~30%–40% of the energy of the primary particle is carried by a leading baryon or nucleus. The remaining energy is employed in the creation of ultra-relativistic secondary particles, most of them charged ($\pi^{\pm}$) and neutral (π^{o}) pions, with a smaller number of hadrons and heavier mesons such as charged and neutral kaons, ρ-mesons, etc.

When primaries of energies of the order of EeV interact with the atmosphere, extended air showers (EAS) are created. They are cascades of millions to billions of secondary particles initiated by a single primary particle. For a primary particle of 10 EeV the lateral spread can be of ~10 km^2 at ground level or more.

Muons

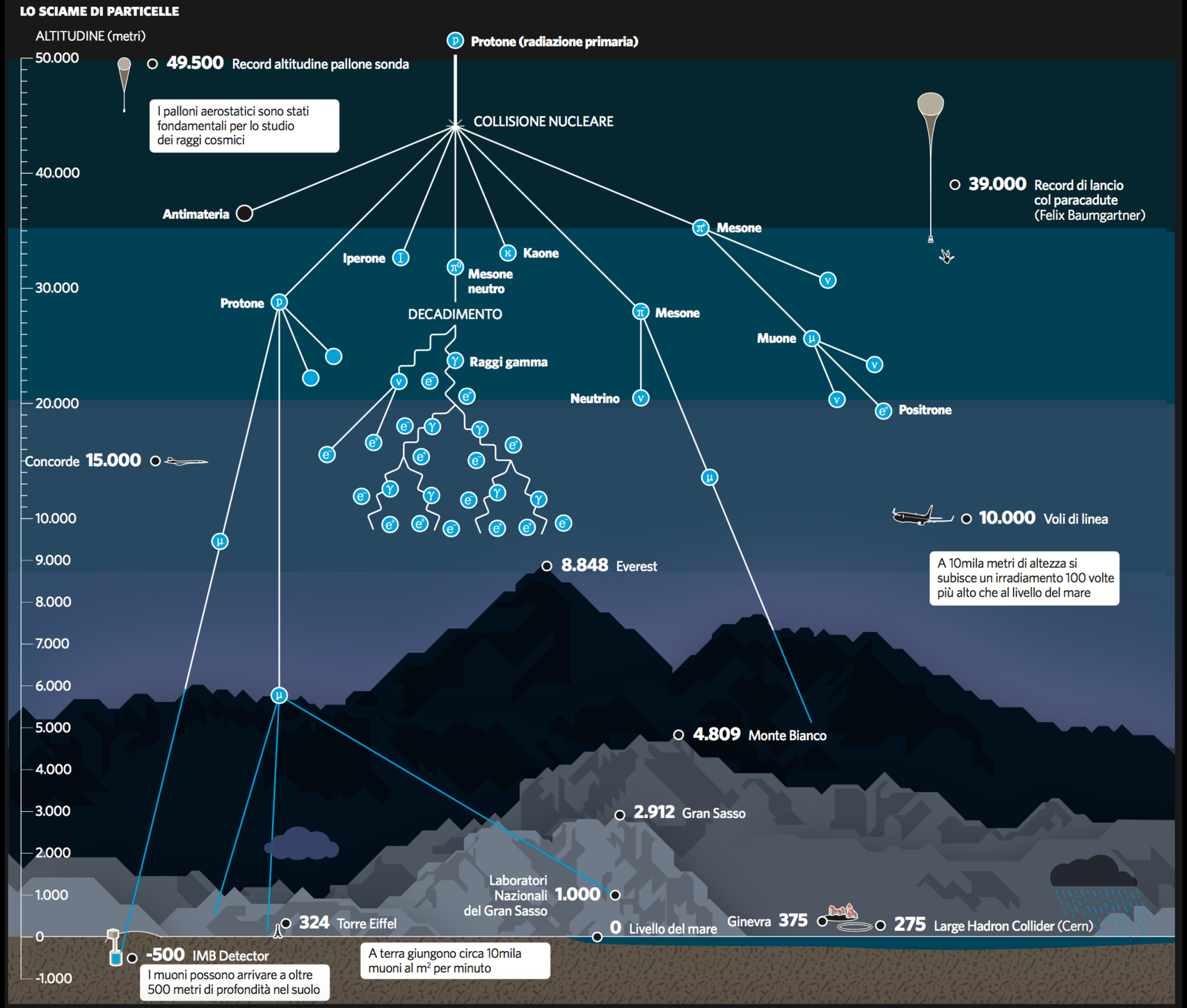
LO SCIAME DI PARTICELLE
ALTITUDINE (metri)
50.000
40.000
30.000
20.000
10.000
9.000
8.000
7.000
6.000
5.000
4.000
3.000
2.000
1.000
0
-1.000
Protone (radiazione primaria)
COLLISIONE NUCLEARE
DECADIMENTO
Antimateria
Iperone
Mesone neutro
Kaone
Mesone
Protone
Mesone
Muone
Raggi gamma
Neutrino
Positrone
49.500 Record altitudine pallone sonda
I palloni aerostatici sono stati fondamentali per lo studio dei raggi cosmici
39.000 Record di lancio col paracadute (Felix Baumgartner)
Concorde 15.000
10.000 Voli di linea
A 10mila metri di altezza si subisce un irradiamento 100 volte più alto che al livello del mare
8.848 Everest
4.809 Monte Bianco
2.912 Gran Sasso
Laboratori Nazionali del Gran Sasso 1.000
324 Torre Eiffel
0 Livello del mare
Ginevra 375
275 Large Hadron Collider (Cern)
-500 IMB Detector
I muoni possono arrivare a oltre 500 metri di profondità nel suolo
A terra giungono circa 10mila muoni al m² per minuto

Charged pions decaying into muons, $\pi^+ = \mu^+ + \nu_\mu$ and $\pi^- => \mu^- +$ (anti)ν_μ, represent the main contribution to the muonic component of the shower (see Figure), being also responsible for the production of the bulk of the so-called atmospheric neutrinos. Most muons of energies above a few GeV travel through the atmosphere without decaying and reach ground

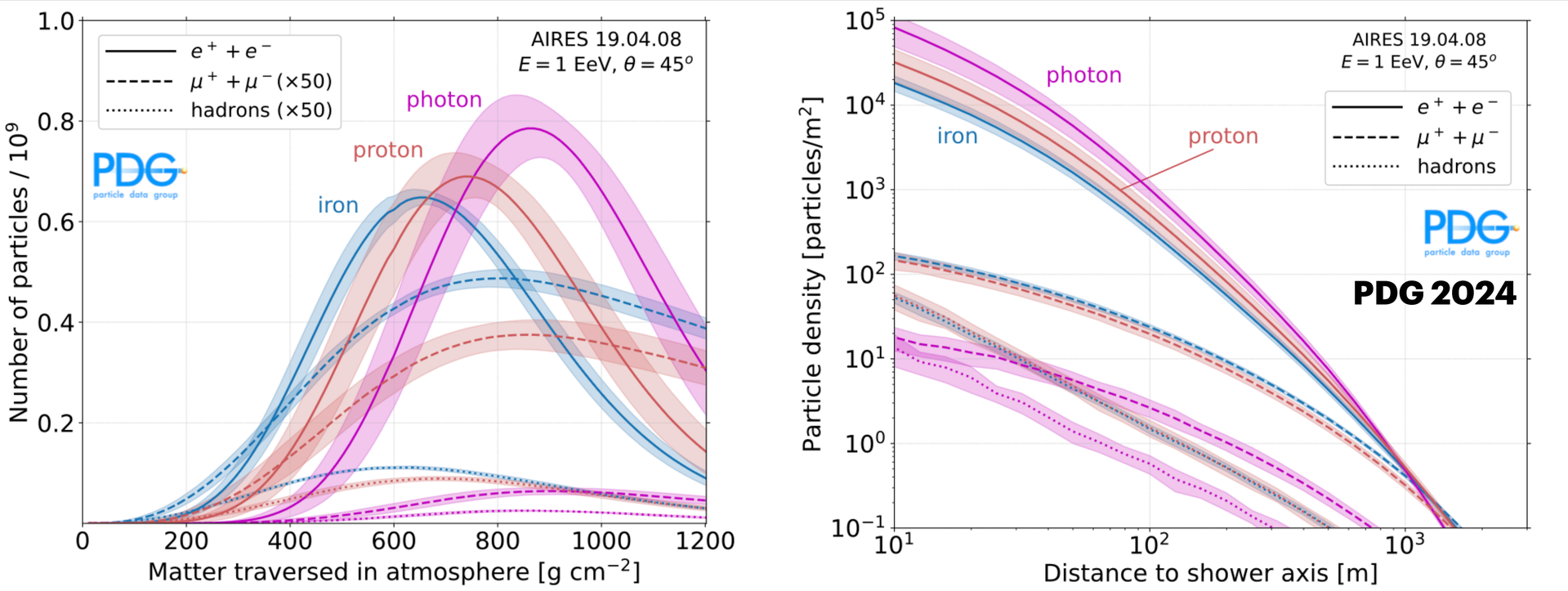

Figure 30.6: Left: Average number of $e^+ + e^-$, $\mu^+ + \mu^-$, and hadrons (lines), and their $\pm 1\,\sigma$ deviation (bands), as a function of matter (in $\mathrm{g\,cm^{-2}}$) crossed in the atmosphere along the shower axis. The profiles are obtained with AIRES simulations [117] of proton, iron and photon-induced extensive air showers of energy $E = 1\,\mathrm{EeV} = 10^{18}\,\mathrm{eV}$ and zenith angle $\theta = 45°$ w.r.t. the vertical to ground (at depth $870\,\mathrm{g\,cm^{-2}}$). Right: Lateral development (perpendicular to shower axis) at ground level of the same components as in the left panel as a function of distance to shower axis.

PDG 2022

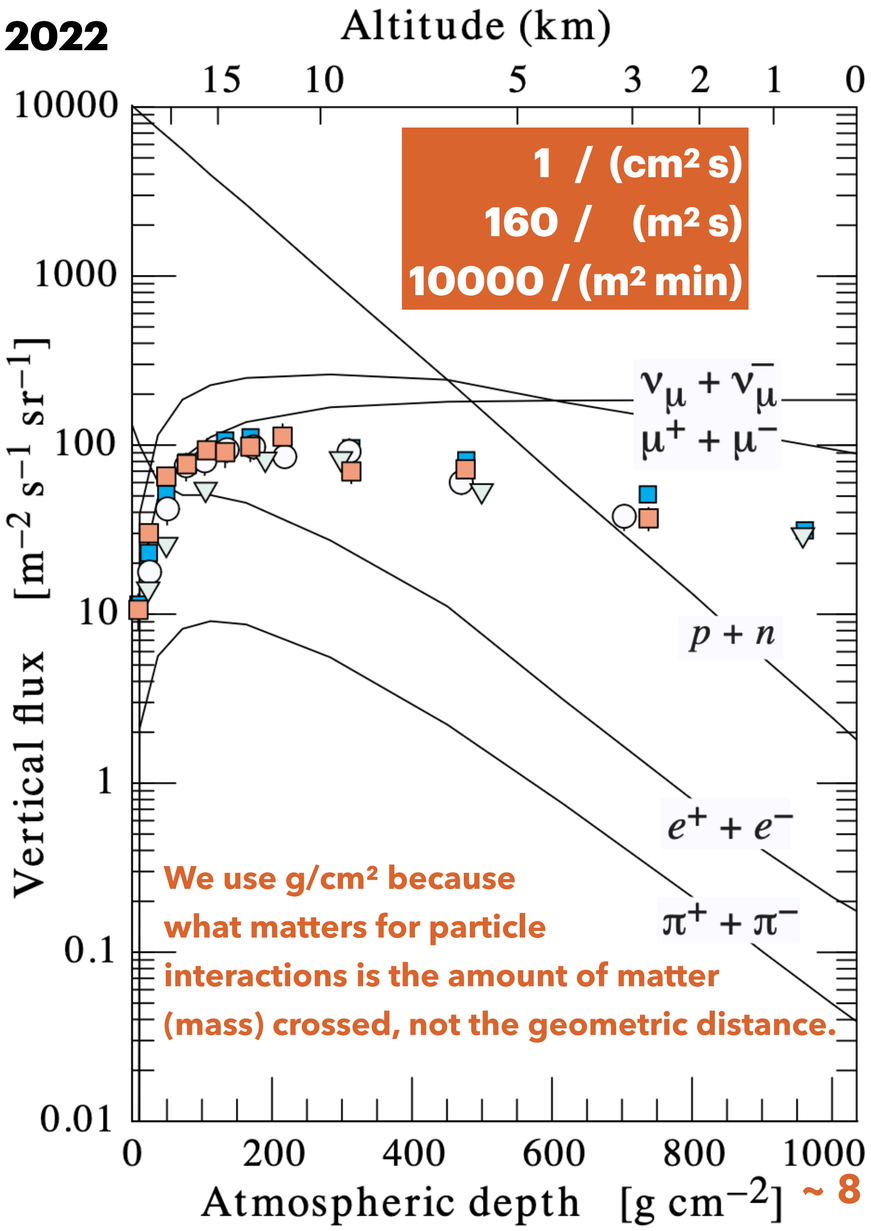

Figure 30.5: Vertical fluxes of cosmic rays in the atmosphere with $E > 1$ GeV estimated from the nucleon flux of Eq. (30.2). The experimental points show measurements of negative muons with $E_\mu > 1$ GeV [57–62].

The integral intensity of vertical muons above 1 GeV/c at sea level is ≈ 70 m^{-2}s^{-1}sr^{-1} [67, 68], with recent measurements [62, 69, 70] favoring a lower normalization by 10-15%. Experimentalists are familiar with this number in the form $I \approx 1$ cm^{-2} min^{-1} for horizontal detectors. The overall angular distribution of muons at the ground as a function of zenith angle θ is $\propto \cos^2\theta$, which is characteristic of muons with $E_\mu \sim 3$ GeV. At lower energy the angular distribution becomes increasingly steep, while at higher energy it flattens, approaching a $\sec\theta$ distribution for $E_\mu \gg \epsilon_\pi$ and $\theta < 70°$.

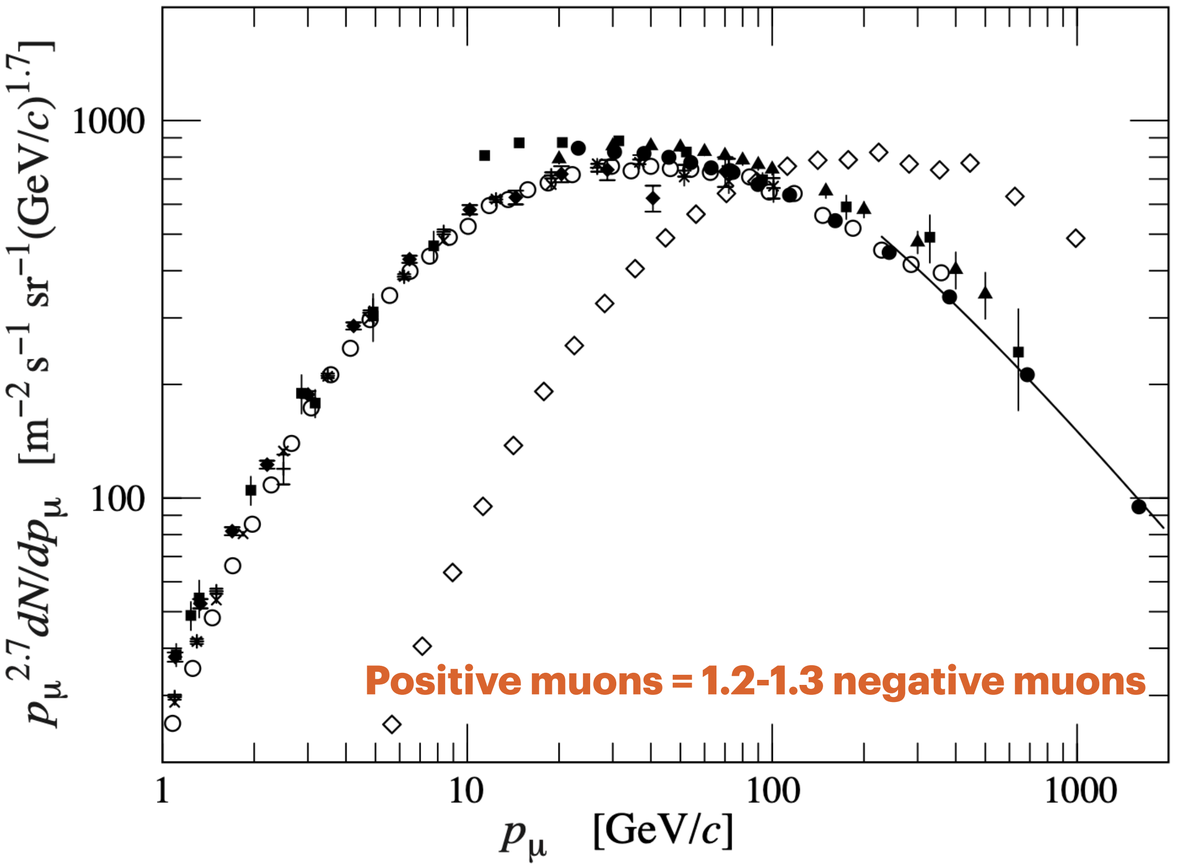

Figure 30.6: Spectrum of muons at $\theta = 0°$ (♦ [67], ■ [71], ▼ [72], ▲ [73], ×, + [69], ○ [62], and • [70] and $\theta = 75°$ ◇ [74]). The line plots the result from Eq. (30.4) for vertical showers.

34.2.3 *Stopping power at intermediate energies*

The mean rate of energy loss by moderately relativistic charged heavy particles is well described by the "Bethe equation" [2,4,5,9],

$$\left\langle -\frac{dE}{dx} \right\rangle = Kz^2 \frac{Z}{A} \frac{1}{\beta^2} \left[\frac{1}{2} \ln \frac{2m_e c^2 \beta^2 \gamma^2 W_{\max}}{I^2} - \beta^2 - \frac{\delta(\beta\gamma)}{2} \right]. \quad (34.5)$$

Eq. (34.5) is valid in the region $0.1 \lesssim \beta\gamma \lesssim 1000$ with an accuracy of a few percent. At $\beta\gamma \sim 0.1$ the projectile speed is comparable to atomic electron "speed," and at $\beta\gamma \sim 1000$ radiative effects begin to be important (Sec. 34.6). Both limits are Z dependent. A minor dependence on M at high energies is introduced through $W_{\max}$, but for all practical purposes the stopping power in a given material is a function of β alone. Small corrections are discussed in Sec. 34.2.6.[1,2]

This is the *mass stopping power*; with the symbol definitions and values given in Table 34.1, the units are MeV $\mathrm{g}^{-1}\mathrm{cm}^2$. As can be seen from Fig. 34.2, dE/dx defined in this way is about the same for most materials, decreasing slowly with Z. The *linear stopping power*, in MeV/cm, is $\rho\, dE/dx$, where ρ is the density in $\mathrm{g/cm}^3$.

Process	Energy regime	Notes
Ionization (Bethe-Bloch)	$\lesssim$ few hundred GeV	Continuous, well-modeled; MIP ~2 MeV $g^{-1}cm^2$
Bremsstrahlung	$\gtrsim$ few hundred GeV	Suppressed by $(m_e/m_\mu)^2$ vs electrons
e^+e^- **pair production**	$\gtrsim$ few hundred GeV	Largest radiative term at high E
Photonuclear	$\gtrsim$ few hundred GeV	Smallest radiative term; stochastic, hard to model
Cherenkov/transition radiation	All energies	Energy loss is negligible but used for **detection**
Muon decay ($\mu \to e\nu\bar{\nu}$)	Low E, long path	Not strictly energy loss but causes muon disappearance

The total energy loss is conventionally written as:

$$-\frac{dE}{dx} = a(E) + b(E) \cdot E$$

where:

- $a(E)$ is the **ionization** term (~2 MeV $g^{-1}cm^2$ in rock, nearly constant)
- $b(E) = b_{\text{brem}} + b_{\text{pair}} + b_{\text{nucl}}$ collects all **radiative** terms (grows linearly with E)

The **critical energy** is defined where the two contributions are equal: $a = b \cdot E_\mu^{\text{crit}}$, giving $E_\mu^{\text{crit}} \approx a/b \sim 500$ GeV in standard rock.

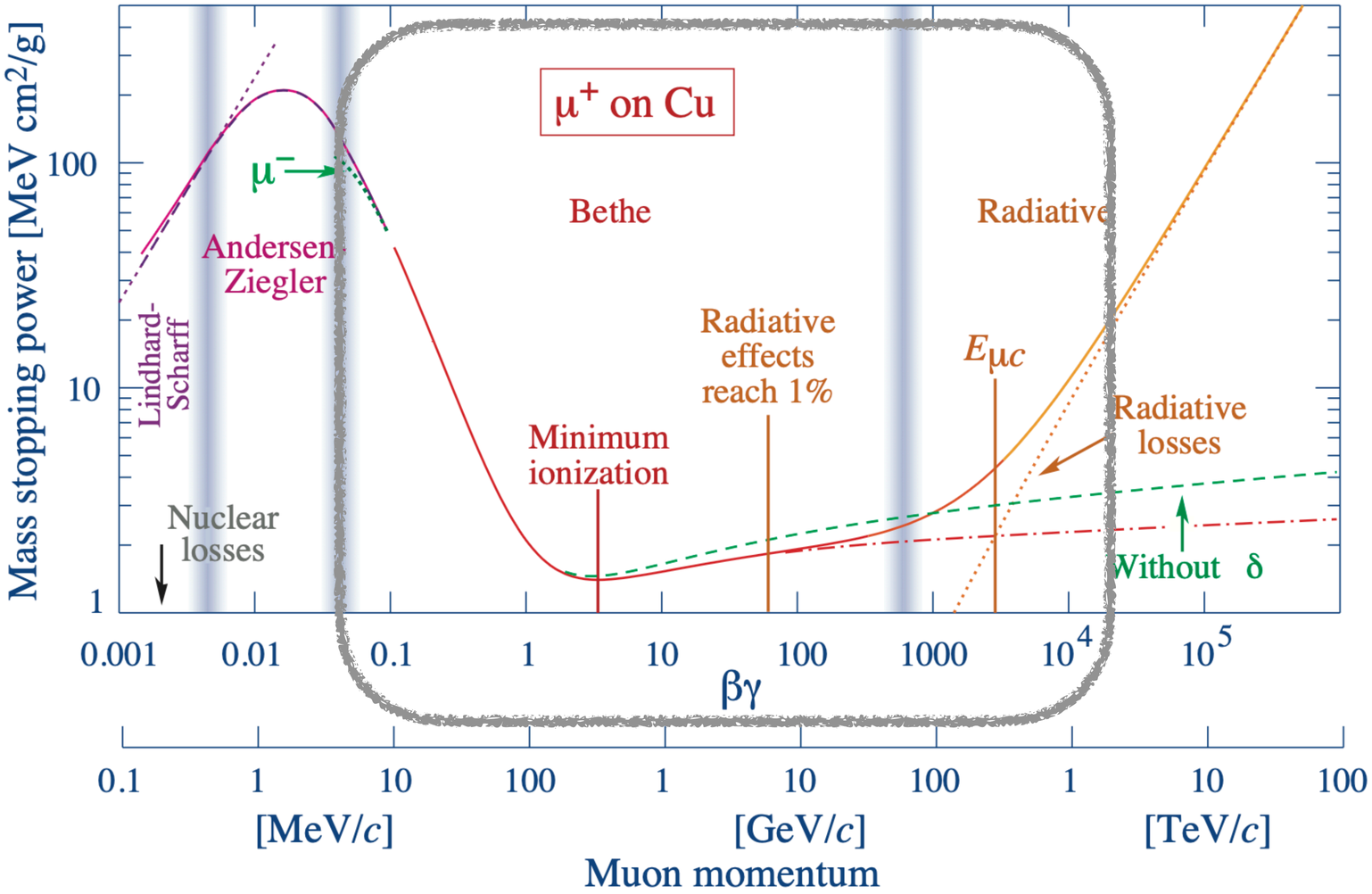

Figure 34.1: Mass stopping power (dE/dx) for positive muons in copper as a function of $\beta\gamma = p/Mc$ over nine orders of magnitude in momentum (12 orders of magnitude in kinetic energy). Solid curves indicate the total stopping power. Data below the break at $\beta\gamma \approx 0.1$ are taken from ICRU 49 [6] assuming only β dependence, and data at higher energies are from [7]. Vertical bands indicate boundaries between different approximations discussed in the text. The short dotted lines labeled "μ^-" illustrate the "Barkas effect," the dependence of stopping power on projectile charge at very low energies [8]. dE/dx in the radiative region is not simply a function of β.

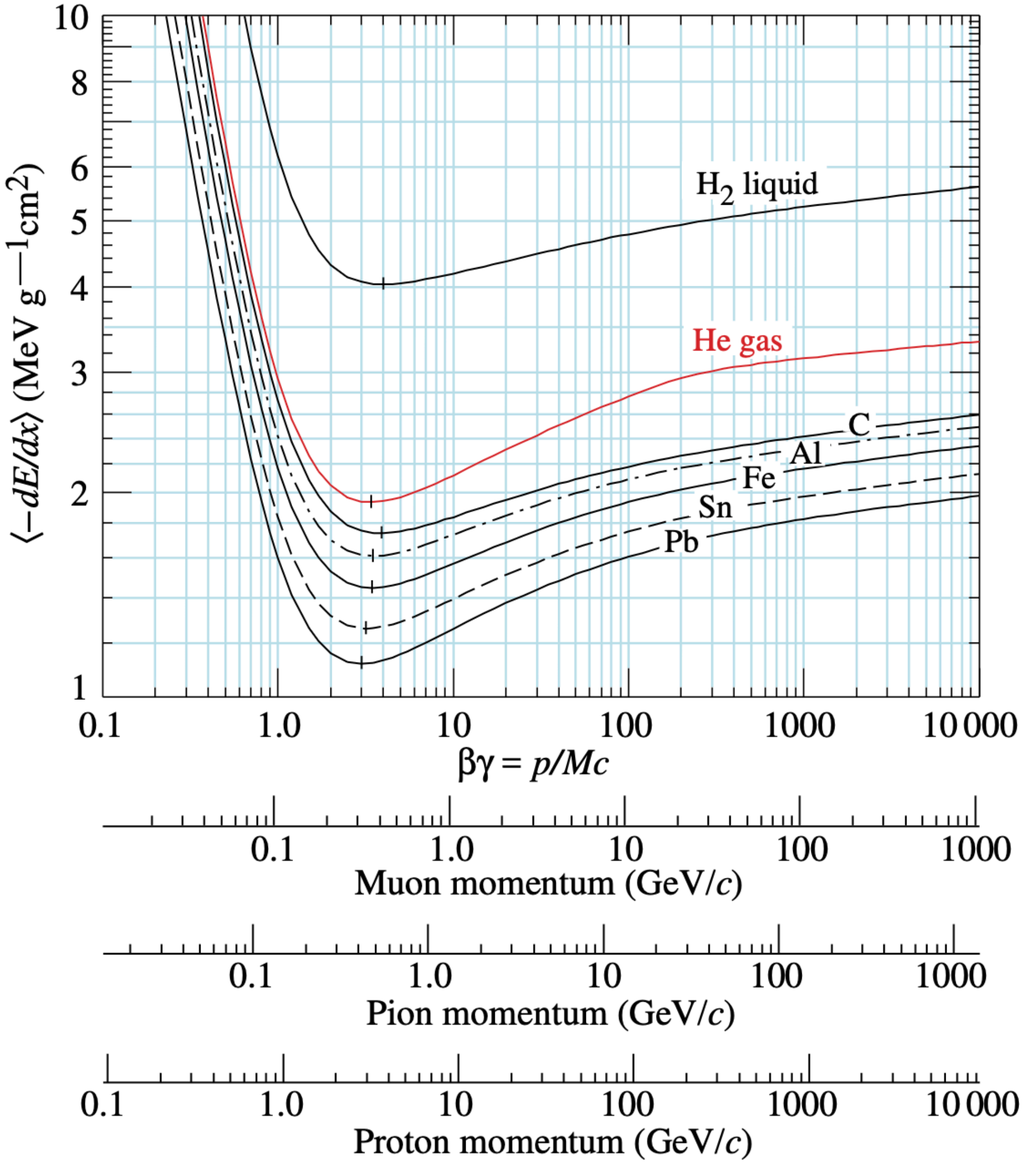

Figure 34.2: Mean energy loss rate in liquid (bubble chamber) hydrogen, gaseous helium, carbon, aluminum, iron, tin, and lead. Radiative effects, relevant for muons and pions, are not included. These become significant for muons in iron for $\beta\gamma \gtrsim 1000$, and at lower momenta for muons in higher-Z absorbers. See Fig. 34.23.

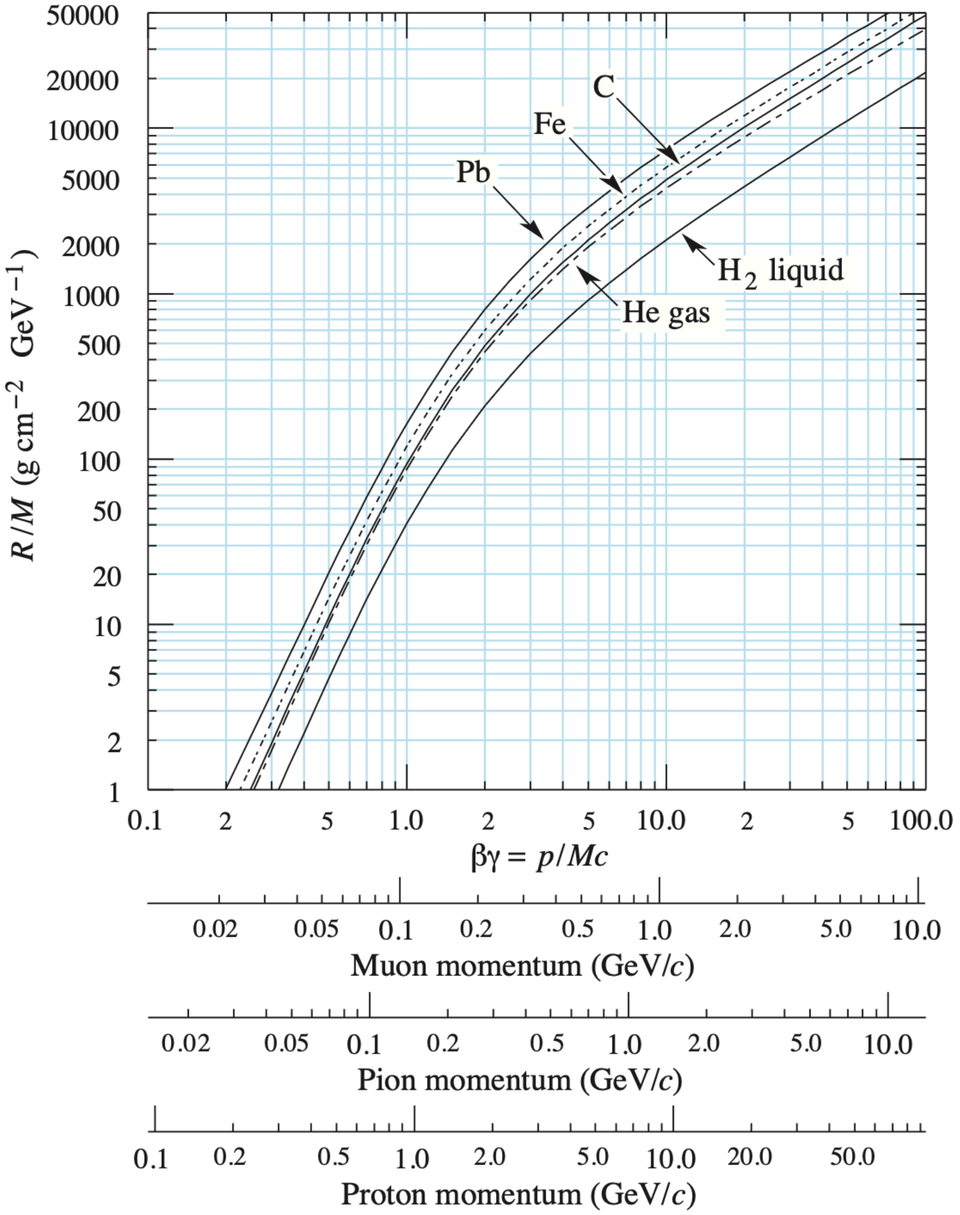

Figure 34.4: Range of heavy charged particles in liquid (bubble chamber) hydrogen, helium gas, carbon, iron, and lead. For example: For a K^+ whose momentum is 700 MeV/c, $\beta\gamma = 1.42$. For lead we read $R/M \approx 396$, and so the range is 195 g cm^{-2} (17 cm).

Some Q&A

Are cosmic ray muons more abundant during the day and less abundant during the night?

No. The differences are negligible.

Does the cosmic ray muons flux depend on the weather?

Yes. The warmer (less dense air) the higher flux (~few %)

Does the cosmic ray muons flux depend on the latitude?

Yes. See Amerigo Vespucci experiment

Are cosmic ray muons more abundant at high altitudes?

Yes. At 2000-3000 m the flux is ~x2 of sea level
At 10000 m the flux is ~ x 10 - x 20
Then it decreases.

scientific reports

Check for updates

OPEN

The Amerigo Vespucci as a traveling laboratory for studying the cosmic-ray fluxes at sea level

Davide Cerasole[1,2], Federica Cuna[1], Gaia De Palma[1,2], Riccardo Di Tria[1], Leonardo Di Venere[1], Fabio Gargano[1], Mario Giliberti[1,2], Francesco Licciulli[1], Antonio Liguori[1,2], Pierpaolo Loizzo[1,3], Francesco Loparco[1,2], Leonarda Lorusso[1], Mario Nicola Mazziotta[1]✉, Giuliana Panzarini[1], Roberta Pillera[1] & Davide Serini[1]

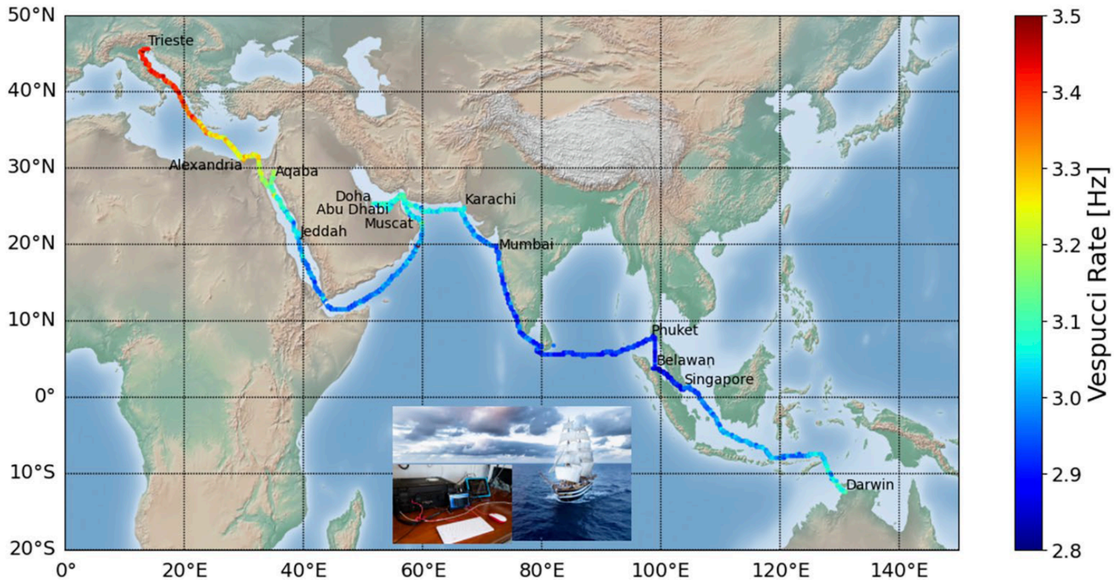

Fig. 1. Cosmic-ray rate map measured on board the Vespucci vessel during its journey from Darwin to Trieste. The color gradient shows the rate values from 2.8 Hz (dark blue) to 3.5 Hz (dark red) with grid spacing resolution of $0.25 \times 0.25\ deg^2$. The cities on the map refer to the main stops of the Vespucci. The map was generated using the Matplotlib Basemap toolkit[14] version 1.4.0 (https://matplotlib.org/basemap/1.4.0/users/index.html).

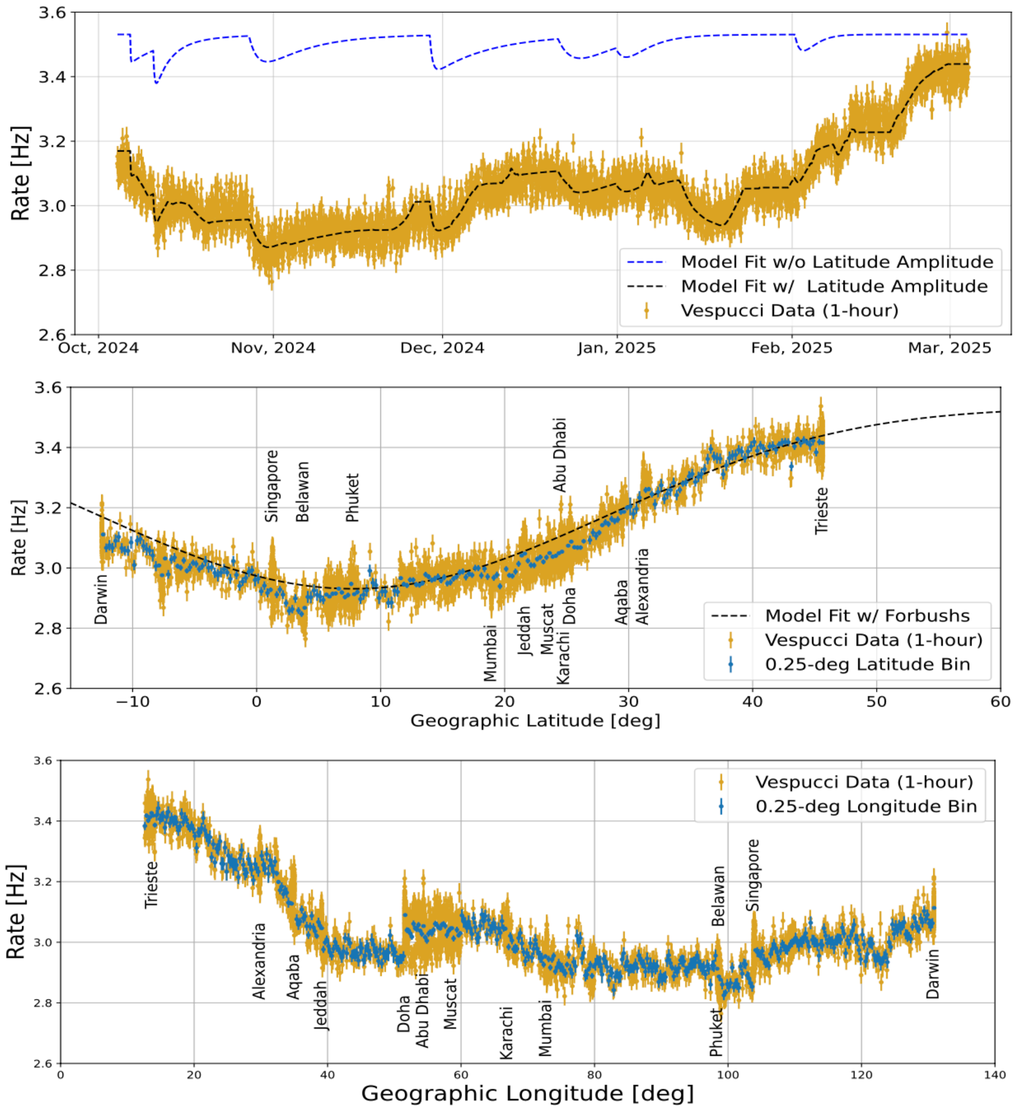

Fig. 2 Top panel: Cosmic-ray rates measured by the detector on board the Vespucci as a function of time since October 4, 2024. Each golden marker corresponds to a 1-hour time interval (UTC time). The dashed black line shows the results of the best fit with Eq. 2. The blue dashed line shows the result of the best fit neglecting the latitude variations (Eq. 2 with the parameter $\alpha = 0$). Middle panel: Cosmic-ray rates as a function of the geographic latitude. The dashed black line is the best fit results with the latitude term of Eq. 2. Bottom panel: Cosmic-ray rates as a function of the geographic longitude. Each golden marker corresponds to a 1-hour time interval. The blue points indicate the average rates evaluated in 0.25° latitude (longitude) bins. The vertical bars represent the statistical errors.

Some Q&A

Are cosmic ray muons more abundant during the day and less abundant during the night?

No. The differences are negligible.

Does the cosmic ray muons flux depend on the weather?

Yes. The warmer (less dense air) the higher flux (~few %)

Does the cosmic ray muons flux depend on the latitude?

Yes. See Amerigo Vespucci experiment

Are cosmic ray muons more abundant at high altitudes?

Yes. At 2000-3000 m the flux is ~x2 of sea level
At 10000 m the flux is ~ x 10 - x 20
Then it decreases.

Cosmic rays make their existence visible?

Yes, during auroras.

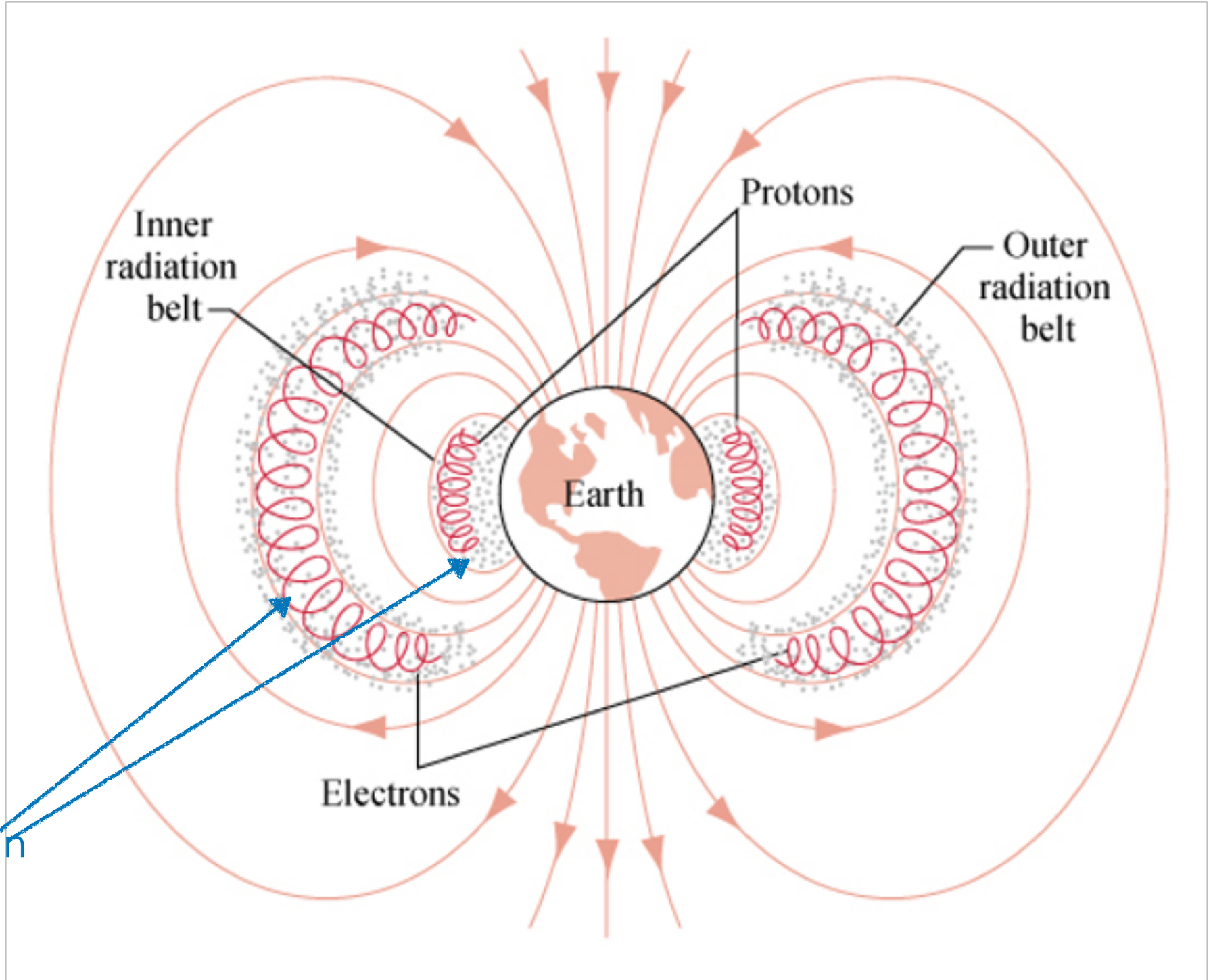
Inner
radiation
belt
Protons
Outer
radiation
belt
Earth
Electrons

Van Allen

Simulations

In particle physics (and consequently also in Muography) we use simulation tools (mostly based on Geant4) to reproduce an experimental setup and extract important informations for the design of the experiment and for the interpretation of the results

BASIC STRUCTURE

```
Primary Generator
        ↓
Physics Processes
        ↓
Tracking Engine (step-by-step)
        ↓
Geometry + Materials interaction
        ↓
Sensitive Detector (energy deposits → hits)
        ↓
Digitization (hits → electronic signals)
        ↓
Output / Analysis
```

GEOMETRY (THE WORLD) AND MATERIALS MODEL

The model must include a full three-dimensional layout (**GEOMETRICAL VOLUME**) of all the “objects” of the experimental setup: the detector, its components, and support structures, everything is around or between them

Material Properties

Each volume is assigned materials with properties that affect particle interactions and energy loss (**PHYSICAL VOLUME**).

Navigation and Boundaries

Geometry defines navigation boundaries for accurate particle tracking across detector regions (**volumes can overlap**).

Fields (electric and magnetic fields)

PHYSICS PROCESSES

Physics List Definition

The physics list defines allowed physical interactions and their modeling during particle simulations.

Categories of Processes

Processes include electromagnetic, hadronic interactions, particle decays, and optical phenomena like scintillation.
For muons, electromagnetic process is generally enough.

Model Selection Criteria

Parameters such as energy thresholds and cutoff must be chosen according to the accuracy of the results (trade-off with CPU speed) [**which is the lower limit after which a particle is neglected/forgotten by the simulation?**].

PRIMARY EVENT GENERATOR (will discuss a little bit more later)

Defines Initial Event Conditions

Primary event generators specify fundamental particle properties, setting initial conditions for each simulated event. Which particle? Which energy? Which origin position? Which energy and geometrical sampling distributions?

Interfaces with Advanced Software

Advanced generators integrate with software modeling physical processes like proton collisions or atmospheric showers.

Ensures Realistic Simulation Accuracy

Careful configuration ensures simulations reflect real experimental conditions including spatial and timing structures.

TRACKING AND STEPPING

Particle Propagation Steps (in the world)

Particle motion is simulated in discrete steps (to be decidåed by user) with evaluations of interactions, energy loss, and scattering [**1 step each MeV? 1 step each 1 cm? = customizable for each particle species**].

Interaction and Decay Processes

The engine decides if particles interact, decay, or continue, generating secondary particles as needed.

Geometry Boundary Handling

Accurate handling of boundaries and material transitions is crucial for modeling detector responses and shielding.

SENSITIVE DETECTORS AND DETECTOR RESPONSE

Role of Sensitive Materials (==> detectors but not necessarily only that)

Sensitive materials identify energy depositions, hit positions, and particle identities inside designated volumes.

Monte Carlo Truth Concept

Monte Carlo truth provides an idealized view of particle interactions without instrument imperfections.

DIGITIZATION

Realistic Signal Simulation

Digitization converts ideal detector hits into realistic electronic signals including noise and time resolution effects.

Detector-Specific Effects

Includes effects like energy resolution, electronic noise, thresholds, saturation, and dead time in the signal modeling.

Conversion and Amplification

Models charge collection, light fluctuations, amplification, and analog-to-digital or time-to-digital conversion processes.

Importance in Data Analysis

Accurate digitization ensures simulated matches experimental data for reliable analysis and performance evaluation.

EVENT RUN AND MANAGEMENT

Event Management Workflow

Event management organizes initialization, execution, and cleanup of single physical occurrences in simulations.

Run Management Control

Run management oversees global settings like random seeds, physics configurations, and output handling.

Parallel Execution Support

Modern frameworks enable parallel execution using multi-core and distributed computing for scalability.

Reproducibility and Reliability

Control of **random number generation** (**SEED**) ensures reproducible and statistically interpretable simulation results.

DATA OUTPUT AND ANALYSIS

Simulation Data Types

Outputs include hit collections, energy depositions, particle trajectories, and truth-level information linking signals to origins.

Standardized Data Formats

Data can be stored in standardized formats like ROOT files to enable efficient analysis and comparison with experiments or in specific user defined formats.

Balancing Completeness and Efficiency

Output structures must optimize between data completeness and storage efficiency to manage large simulation volumes.

Geant4

Toolkit for the simulation of the passage of particles through matter. Its areas of application include high energy, nuclear and accelerator physics, as well as studies in medical and space science.

Getting started

All the physics about the interaction of muons with matter is included in a simulation package developed at CERN and called GEANT4. Indeed GEANT4 is a toolkit for **simulating the passage of particles through matter**. It includes a complete range of functionality including **tracking, geometry, physics models and hits**.

The toolkit is the result of a worldwide collaboration of physicists and software engineers. It has been created exploiting software engineering and object-oriented technology and implemented in the C++ programming language. It is being used in applications in particle physics, nuclear physics, **applied physics**, accelerator design, space engineering and medical physics.

It is the most complete, reliable and basically the de facto statutory toolkit for simulations of cosmic-ray applications

Get started

Everything you need to get started with Geant4.

I'm ready to start!

Download

Geant4 source code and installers are available for download, with source code under an open source license.

Latest: 11.4.1

Docs

Documentation for Geant4, along with tutorials and guides, are available online.

Read documentation

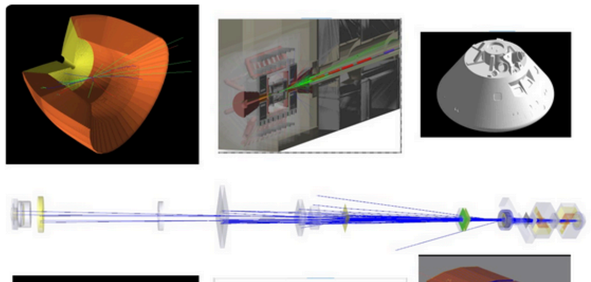

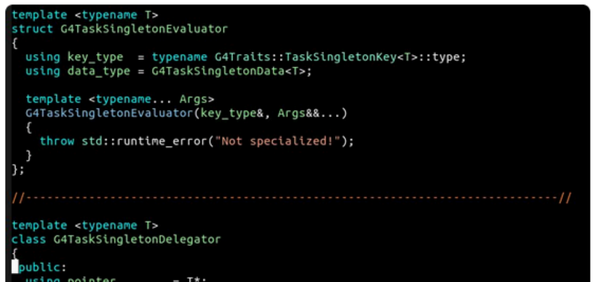

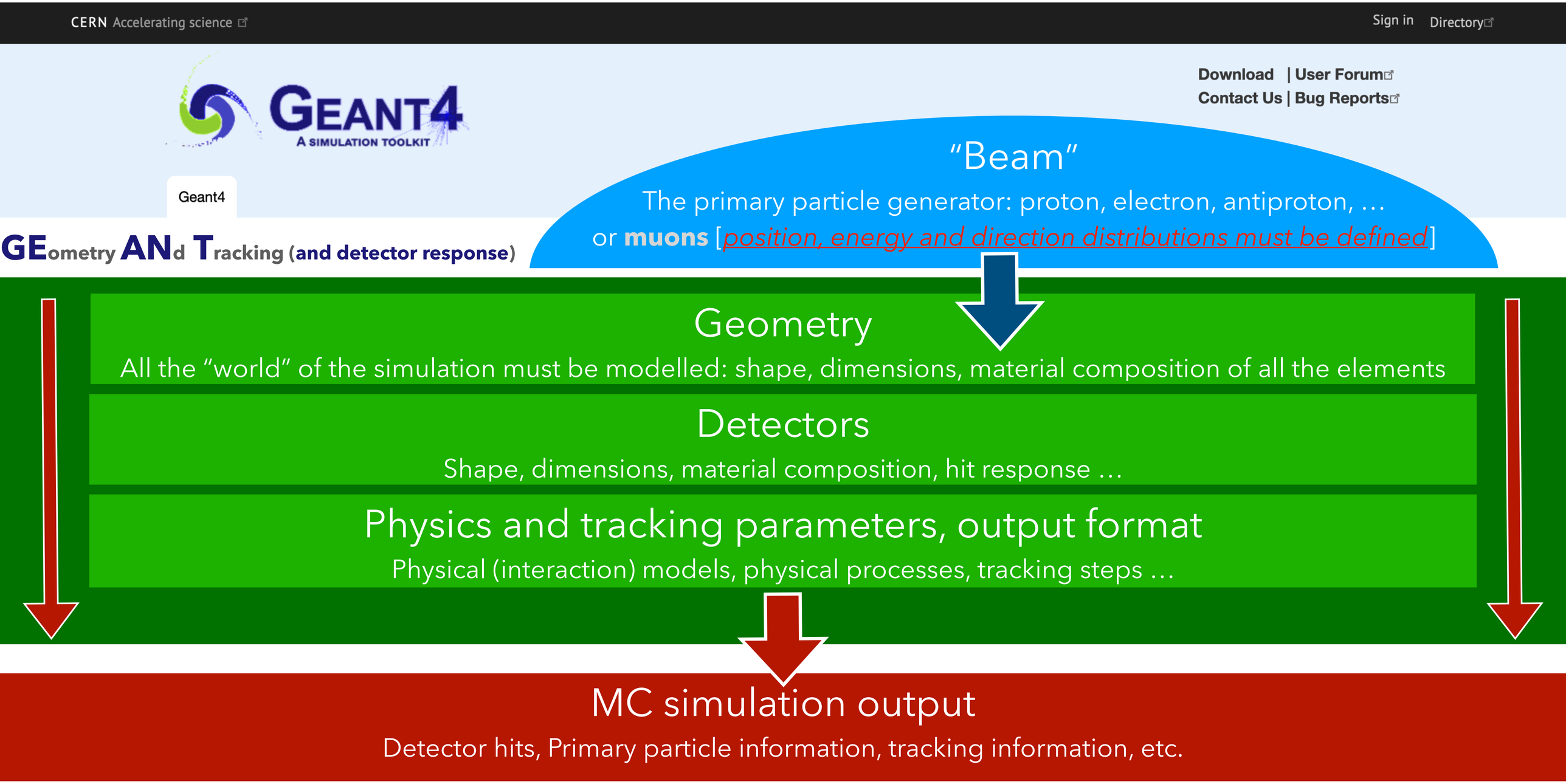
CERN Accelerating science
Sign in
Directory
GEANT4
A SIMULATION TOOLKIT
Download | User Forum
Contact Us | Bug Reports
Geant4
GEometry ANd Tracking (and detector response)
"Beam"
The primary particle generator: proton, electron, antiproton, …
or muons [position, energy and direction distributions must be defined]
Geometry
All the "world" of the simulation must be modelled: shape, dimensions, material composition of all the elements
Detectors
Shape, dimensions, material composition, hit response …
Physics and tracking parameters, output format
Physical (interaction) models, physical processes, tracking steps …
MC simulation output
Detector hits, Primary particle information, tracking information, etc.

Muon generators

Even though many applications in muon radiography and tomography rely on custom-made codes for the generation of CR muons, several tools for this task are currently available. Among them, we can perform the following coarse classification:

- cosmic-ray air shower (CRAS) generators

simulate the full cascade of secondary particles initiated by primary cosmic rays;

- parametric generators

using a parametrization of the flux of CR muons, based either on experimental data or on the results from simulations with CRAS generators;

- special generators

specifically designed for underground, high altitude or underwater experiments

Cosmic-ray air shower (CRAS) generators

CORSIKA

CRY

AIRES

Parametric generators

GEMC

CMSCGEN

EcoMug

Special generators

MuTev

MUPAGE

Custom generators

...

...

Transmission Muography applications are sensitive to the **angular distribution** of muons, and many applications of **scattering muography** are also sensitive to their **momentum distribution**. For these reasons, an accurate simulation of the dependency of the muon flux on momentum and direction is a key requirement for every generation tool targeting to such applications.

Moreover, as the inspection of large structures requires a very large statistics, **the generator has also to be (reasonably) fast**.

EcoMug

Nuclear Inst. and Methods in Physics Research, A 1014 (2021) 165732

Contents lists available at ScienceDirect

Nuclear Inst. and Methods in Physics Research, A

journal homepage: www.elsevier.com/locate/nima

1-5 JUNE BUDAPEST Muographers 2026

https://dr4kan.github.io/EcoMug/index.html

EcoMug: An Efficient COsmic MUon Generator for cosmic-ray muon applications

D. Pagano [a,b,*], G. Bonomi [a,b], A. Donzella [a,b], A. Zenoni [a,b], G. Zumerle [c,d], N. Zurlo [e,b]

[a] Department of Mechanical and Industrial Engineering, University of Brescia, Italy
[b] Istituto Nazionale di Fisica Nucleare (INFN), Pavia, Italy
[c] Department of Physics and Astronomy, University of Padova, Padova, Italy
[d] Istituto Nazionale di Fisica Nucleare (INFN), Padova, Italy
[e] Department of Civil, Environmental, Architectural Engineering and Mathematics, University of Brescia, Italy

Check for updates

EcoMug: Efficient COsmic MUon Generator

EcoMug is a header-only C++11 library for the generation of cosmic ray (CR) muons, based on a parametrization of experimental data. Unlike other tools, EcoMug gives the possibility of generating from different surfaces (plane, cylinder and half-sphere), while keeping the correct angular and momentum distribution of generated tracks. EcoMug also allows the generation of CR muons according to user-defined parametrizations of their differential flux.

If you use, or want to refer to, EcoMug please cite the following paper:

> Pagano, D., Bonomi, G., Donzella, A., Zenoni, A., Zumerle, G., & Zurlo, N. (2021). EcoMug: An Efficient COsmic MUon Generator for cosmic-ray muon applications. Nuclear Instruments and Methods in Physics Research Section A: Accelerators, Spectrometers, Detectors and Associated Equipment, 1014, 165732.

Latest release: EcoMug v2.0.0

In EcoMug, the origin points of generated muons can be sampled from a **plane surface** (flat sky generation), from a **cylindrical surface** or from a **half-spherical surface**, while keeping the correct angular and momentum distributions.

The three generations are equivalent (in terms of “physics”)

Differential flux

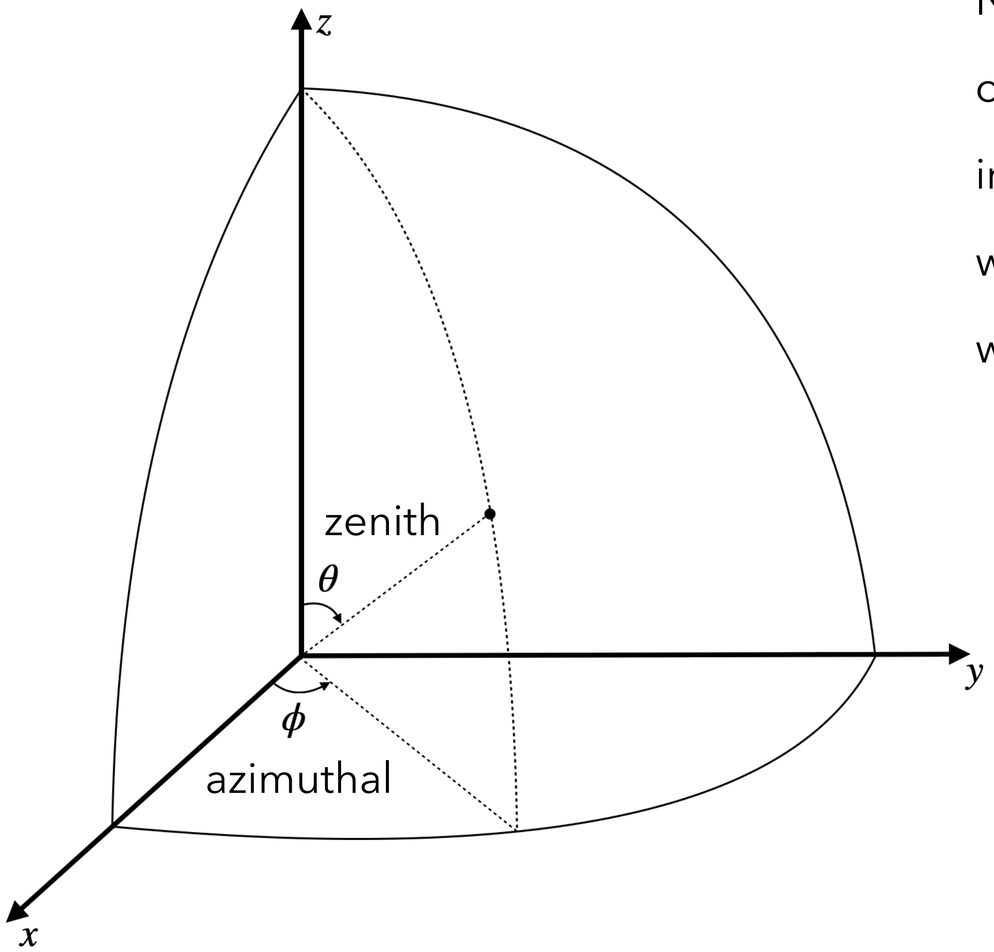

Number of cosmic-ray muons

crossing a surface dS_n **perpendicular to the muon direction**

in a interval of time dt

with momentum between p and p+dp,

within a dΩ solid angle around the direction (θ, Φ)

$$J \equiv J(t, p, \theta, \phi) = \frac{dN}{dt \cdot dp \cdot d\Omega \cdot dS_n}$$

being $d\Omega = \sin\theta \; d\theta \; d\phi$ we can also write

$$J \equiv J(t, p, \theta, \phi) = \frac{dN}{dt \cdot dp \cdot \sin\theta \cdot d\theta \cdot d\phi \cdot dS_n}$$

Angular and momentum distributions - EcoMug

The distributions of momentum and arrival direction of the muons in the simulation must be as close as possible to the "real"(*) one.

L. Bonechi, M. Bongi, D. Fedele, M. Grandi, S. Ricciarini, E. Vannuccini,
Development of the ADAMO detector: test with cosmic rays at different zenith angles,
in: 29th International Cosmic Ray Conference Vol. 9, 2005, pp. 283.

$$J = \left[1600 \cdot \left(\frac{p}{p_0} + 2.68\right)^{-3.175} \cdot \left(\frac{p}{p_0}\right)^{0.279}\right] \cdot (\cos\theta)^n \cdot \frac{1}{\mathrm{m}^2 \cdot \mathrm{s} \cdot \mathrm{sr} \cdot \mathrm{GeV/c}}$$

L. Bonechi, Misure di Raggi Cosmici a Terra con l'Esperimento ADAMO (Ph.D. thesis), Università degli Studi di Firenze, Dipartimento di Fisica, 2004.

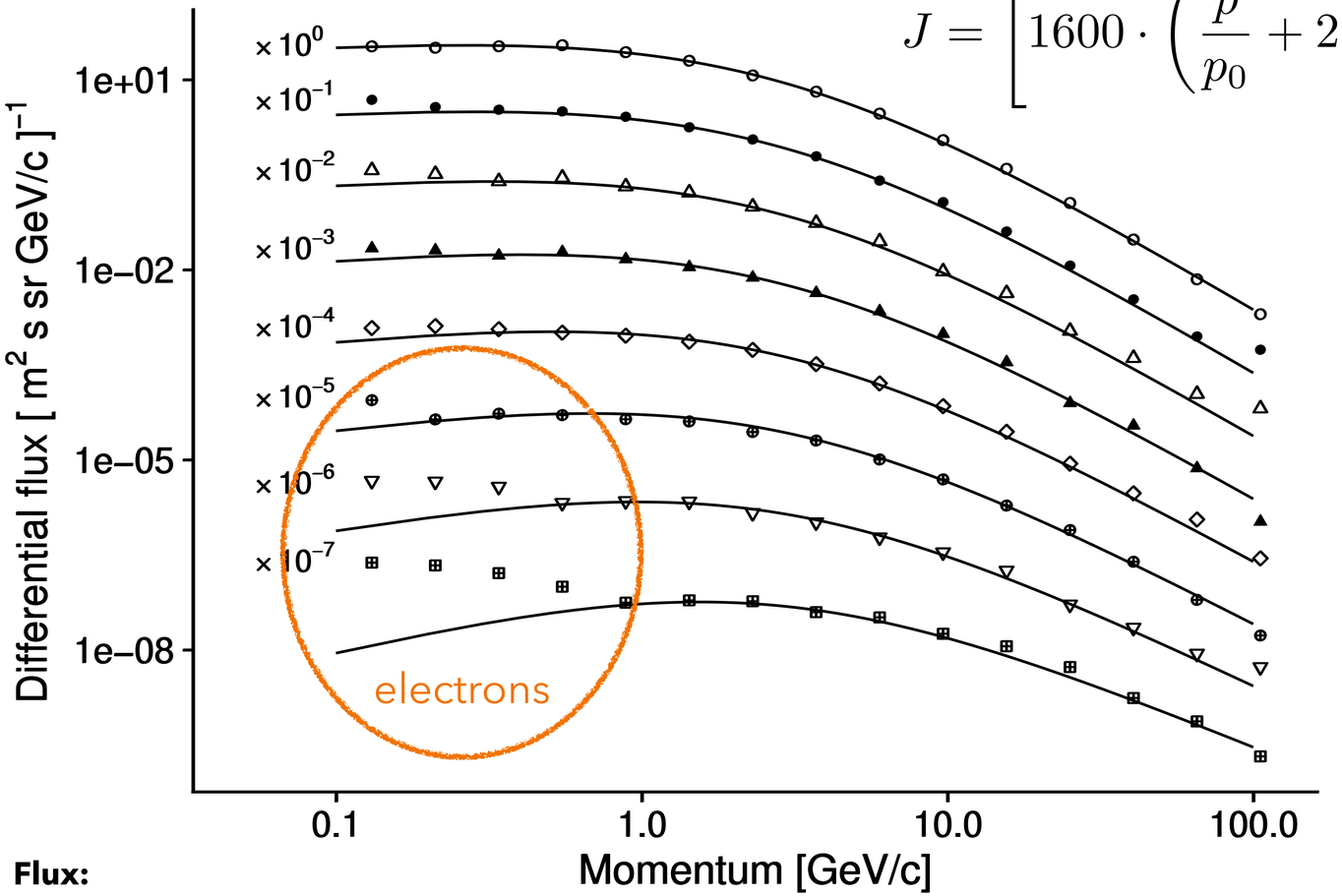

- ○ 0° < θ < 10°
- ● 10° < θ < 20°
- △ 20° < θ < 30°
- ▲ 30° < θ < 40°
- ◇ 40° < θ < 50°
- ⊕ 50° < θ < 60°
- ▽ 60° < θ < 70°
- ⊞ 70° < θ < 80°

with $p_0 = 1\ \mathrm{GeV/c}$

$p > 0.040\ \ \mathrm{GeV/c}$

and $n(p) = \max\left[0.1,\ 2.856 - 0.655 \cdot \ln\left(\frac{p}{p_0}\right)\right]$

Flux:
integral over momentum and angle for a horizontal surface: **125 u/(m² s)**
integral over momentum and angle for a vertical surface: **60 u/(m² s) [both sides]**
Important to compute "real world data taking time equivalent" of simulations

*EcoMug generated muons with momentum **up to 1000 GeV/c and zenith angles up to 90°**. The user should keep in mind, though, that the above equation **could not describe accurately the flux outside the range of experimental data**, even though this can be fixed by resorting to reweighting techniques*

(*) Clearly there are no "ones for all real distributions". The momentum, arrival direction and flux may depend on many parameters: solar activity, altitude, air temperature and pressure, etc. etc.

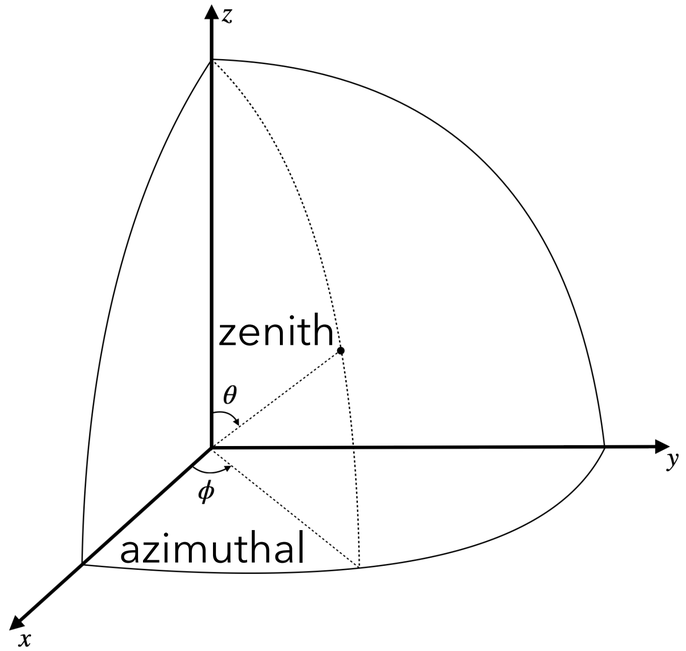

Monte Carlo generations

It is more functional to consider the following:

(A different definition of) differential flux (J')

Number of cosmic-ray muons

crossing a ***surface dS_n perpendicular to the muon direction***

in a interval of time dt

with momentum between p and p+dp

with zenith angle between θ and θ + dθ

with azimuthal angle between Φ and Φ + dΦ,

$$J' = \frac{dN}{dt \cdot dp \cdot d\theta \cdot d\phi \cdot dS_n}$$

$$J \equiv J(t,p,\theta,\phi) = \frac{dN}{dt \cdot dp \cdot d\Omega \cdot dS_n} \qquad d\Omega = \sin\theta \; d\theta \; d\phi \qquad J' = \frac{dN}{dt \cdot dp \cdot d\theta \cdot d\phi \cdot dS_n} = J(t,p,\theta,\phi) \cdot sin\theta$$

$$J' = \left[1600 \cdot \left(\frac{p}{p_0} + 2.68 \right)^{-3.175} \cdot \left(\frac{p}{p_0} \right)^{0.279} \right] \cdot (\cos\theta)^n \cdot sin\theta \cdot \frac{1}{\mathrm{m}^2 \cdot \mathrm{s} \cdot \mathrm{sr} \cdot \mathrm{GeV/c}}$$

1-5 JUNE BUDAPEST Muographers 2026

a) flux with respect to an horizontal surface

2D simplification

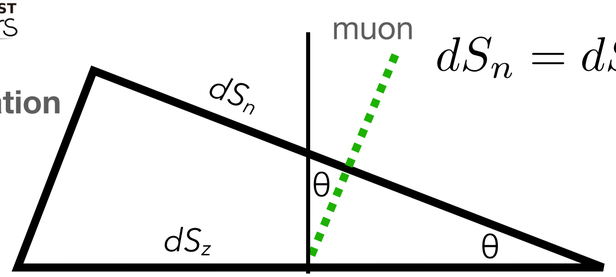

$$dS_n = dS_z \cdot \cos\theta$$

$$J'_z \equiv \frac{dN}{dt \cdot dp \cdot d\theta \cdot d\phi \cdot dS_z} = \left[1600 \cdot \left(\frac{p}{p_0} + 2.68\right)^{-3.175} \cdot \left(\frac{p}{p_0}\right)^{0.279}\right] \cdot (\cos\theta)^{n+1} \cdot \sin\theta \cdot \frac{1}{\mathrm{m}^2 \cdot \mathrm{s} \cdot \mathrm{sr} \cdot \mathrm{GeV/c}}$$

b) flux with respect to a vertical surface

$$J'_x \equiv \frac{dN}{dt \cdot dp \cdot d\theta \cdot d\phi \cdot dS_x} = \left[1600 \cdot \left(\frac{p}{p_0} + 2.68\right)^{-3.175} \cdot \left(\frac{p}{p_0}\right)^{0.279}\right] \cdot (\cos\theta)^{n} (\sin\theta)^2 \cos\phi \cdot \frac{1}{\mathrm{m}^2 \cdot \mathrm{s} \cdot \mathrm{sr} \cdot \mathrm{GeV/c}}$$

2D simplification

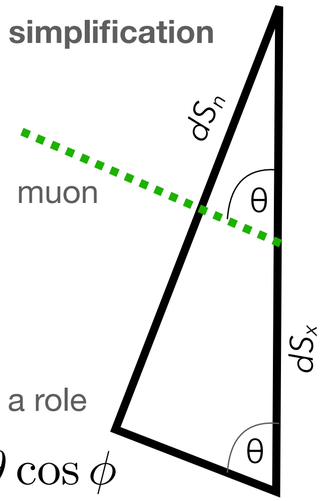

Cylinder lateral surface => also Φ plays a role

$$dS_n = dS_x \; \hat{x} \cdot \hat{n} = dS_x \sin\theta \cos\phi$$

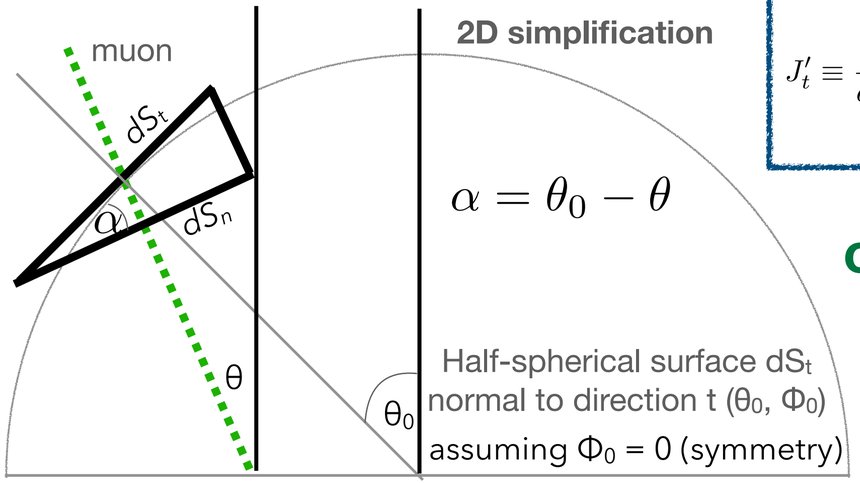

2D simplification

$$\alpha = \theta_0 - \theta$$

Half-spherical surface dS_t normal to direction t (θ_0, Φ_0) assuming Φ_0 = 0 (symmetry)

$$J'_t \equiv \frac{dN}{dt \cdot dp \cdot d\theta \cdot d\phi \cdot dS_t} = \left[1600 \cdot \left(\frac{p}{p_0} + 2.68\right)^{-3.175} \cdot \left(\frac{p}{p_0}\right)^{0.279}\right] \cdot (\cos\theta)^{n} \left[\sin\theta_0 (\sin\theta)^2 \cos\phi + \cos\theta_0 \cos\theta \sin\theta\right] \cdot \frac{1}{\mathrm{m}^2 \cdot \mathrm{s} \cdot \mathrm{sr} \cdot \mathrm{GeV/c}}$$

c) flux with respect to a “infinitesimal” hemispherical surface

$$dS_n = dS_t \; \hat{t} \cdot \hat{n} = dS_t \left[\sin\theta_0 \sin\theta \cos\phi + \cos\theta_0 \cos\theta\right]$$

Generation over a flat sky (horizontal surface)

To generate all the useful cosmic-ray muons, one would need an “infinite” flat sky => cumbersome in terms of computing

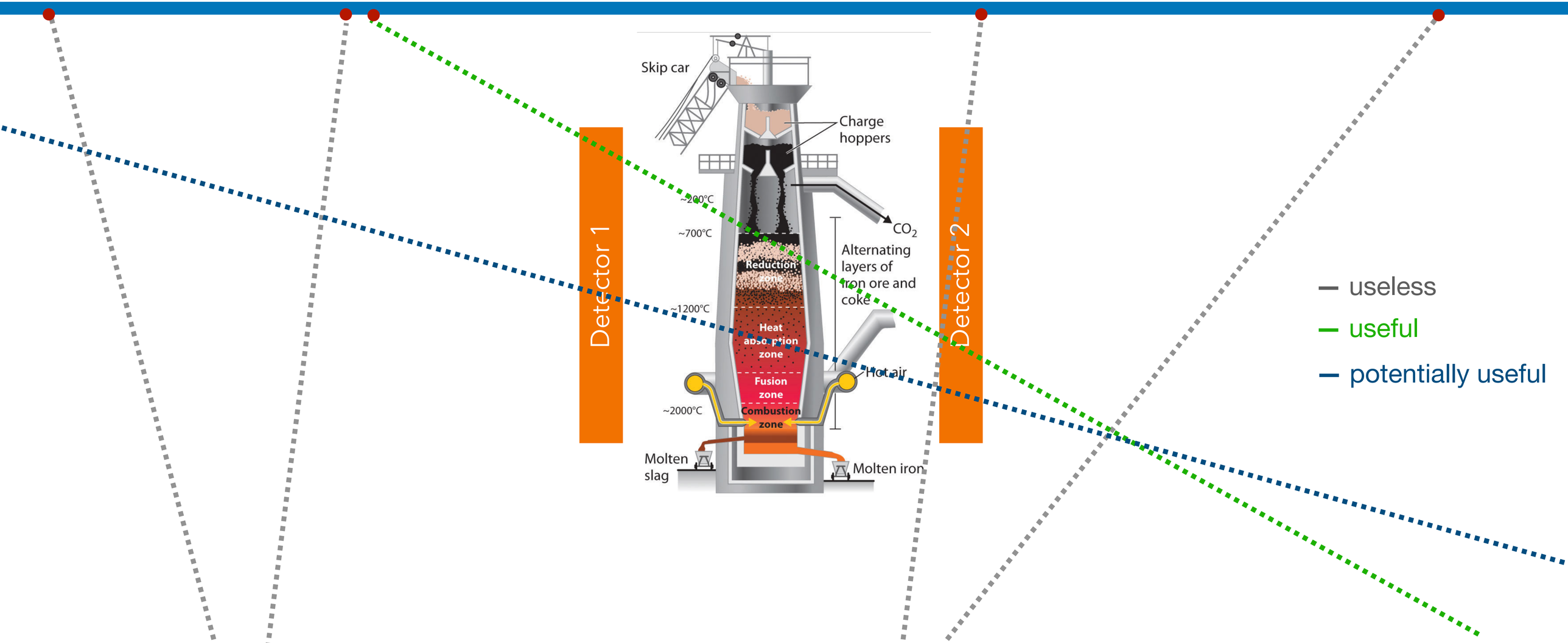

Generation over a cylindrical (lateral) surface

For muon tomography of large and tall structures, generation over a cylinder becomes much more efficient

EcoMug can generate over a:

- **horizontal** surface
  [flat sky generation]
- **cylinder lateral** surface
  [cylindrical generation]
- **hemispherical** surface
  [half-spherical generation]

... the generation of a muon in EcoMug involves the use of the acceptance–rejection method in a 2D space, for a flat sky and cylindrical surface, and in a 4D space, for the half-spherical surface, to sample according to the distributions described in the following ...

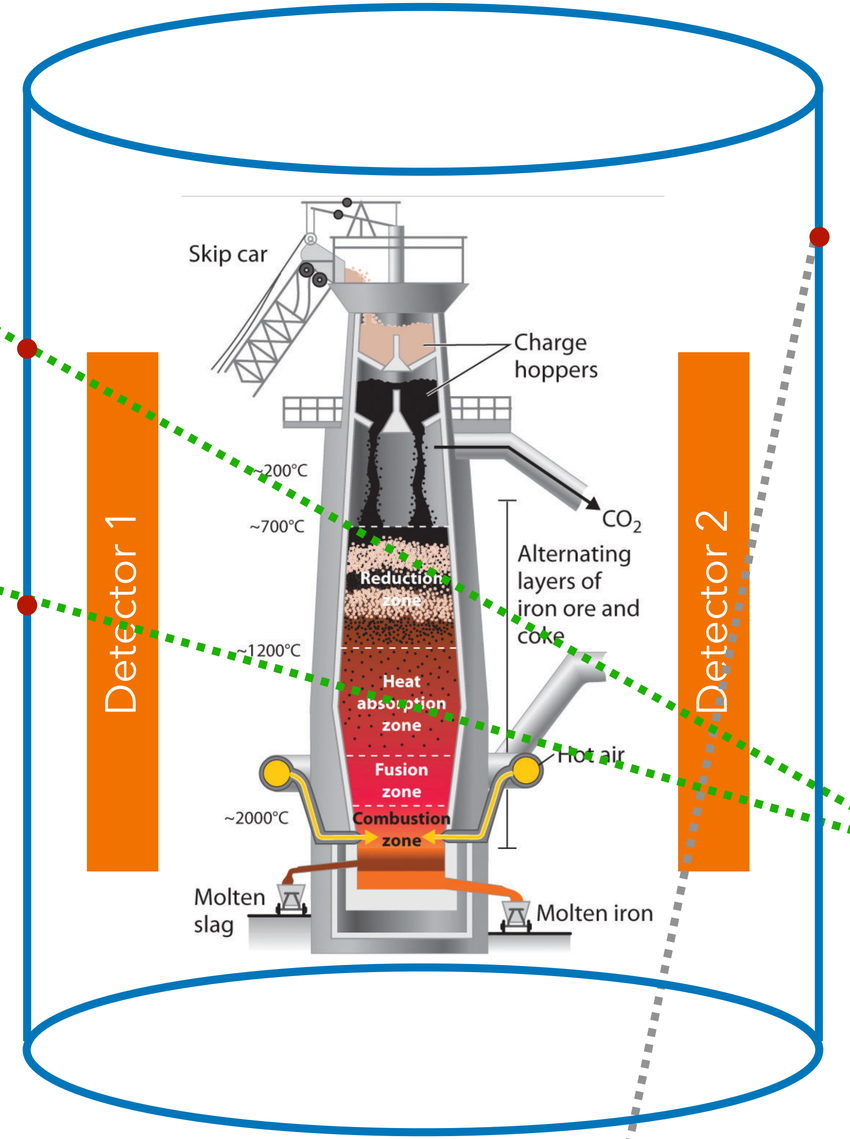

Since the statistics are large in these Monte Carlo simulations, a very fast and reliable pseudo-random number generator (PRNG) is useful. EcoMug internally uses a class called EMRandom, which is based on the xoroshiro128+ algorithm, the fastest PRNG algorithm.
The time required to generate 1M muons, using a compiled code with the -O3 flag on a 2.6 GHz Intel Core i7 6 core, was on average:

- **1.3 s for the flat sky generator;**
- **2.6 s for the cylindrical generator**
- **4.9 s for the half-sphere generator**

— useless

— useful

Example 1: “vertical” detectors

- we generate over a cylindrical and a half-spherical surface
- we require the muon to cross both vertical detectors
- we compare the distributions of p, θ and Φ (filtered by the two detectors)

4. Comparison between the different generation methods

The generation methods discussed above, and implemented in Eco-Mug, are mathematically equivalent, provided that all of them grant the proper coverage of the geometrical acceptance of the detection system. However, depending on the case study, one method could be more effective than the others, in respect to the generation time. In this section, a comparison of the performance of the three generation methods, for three different scenarios, is presented.

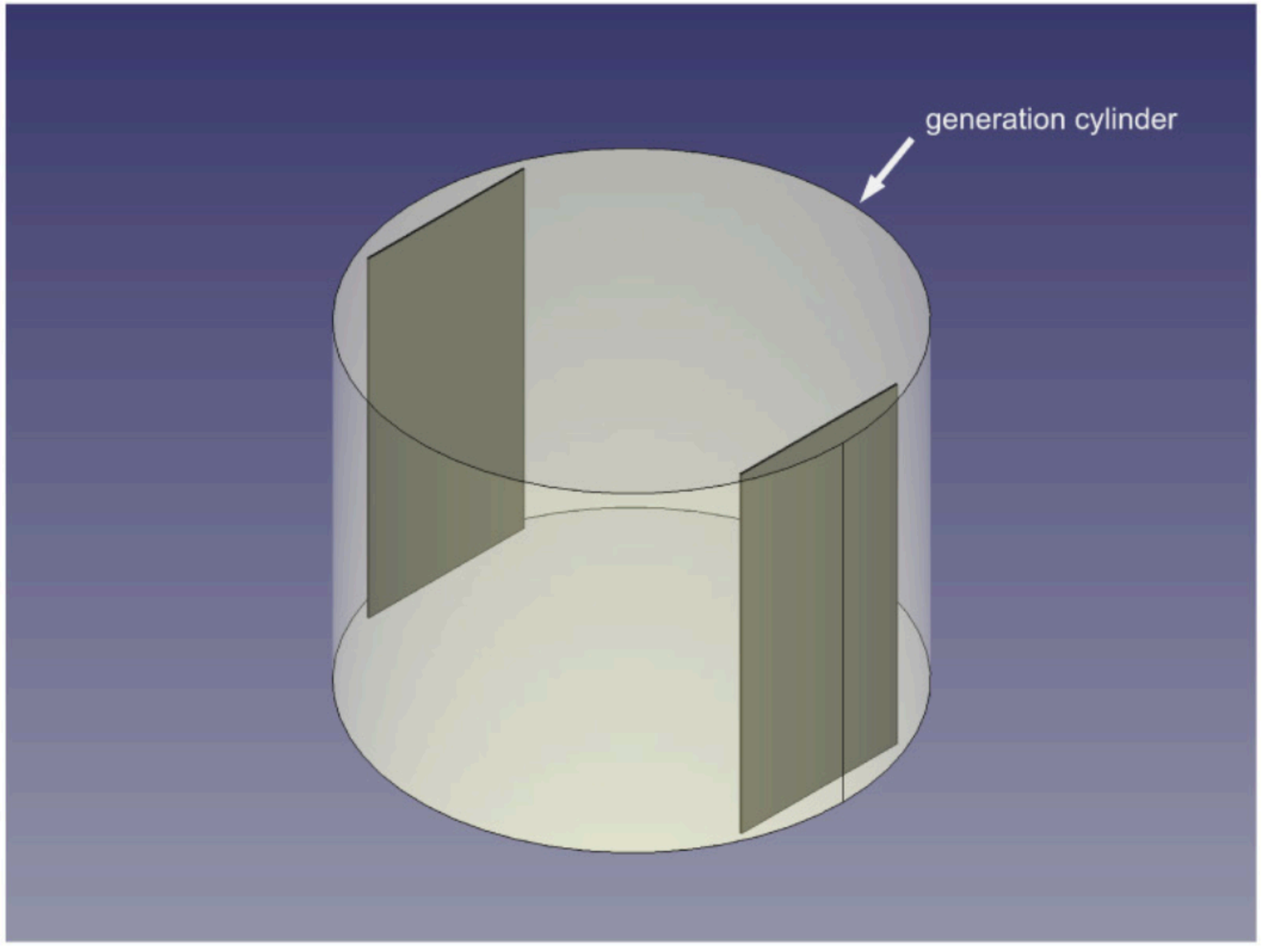

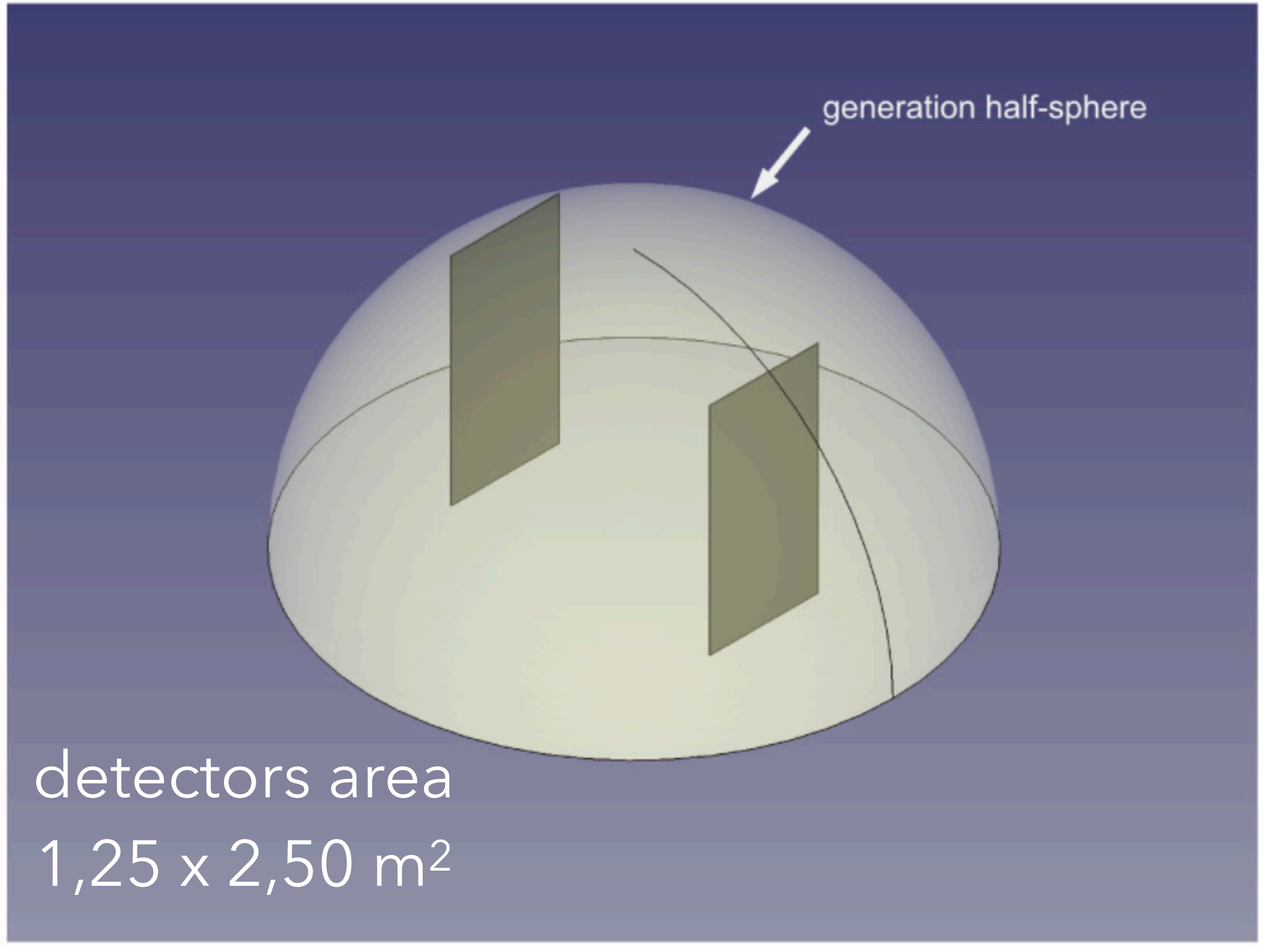

Example 2: a muon telescope

- we generate over a flat sky and a half-spherical surface
- we require the muon to cross all the three horizontal detectors
- we compare the distributions of p, θ and Φ (filtered by three detectors)

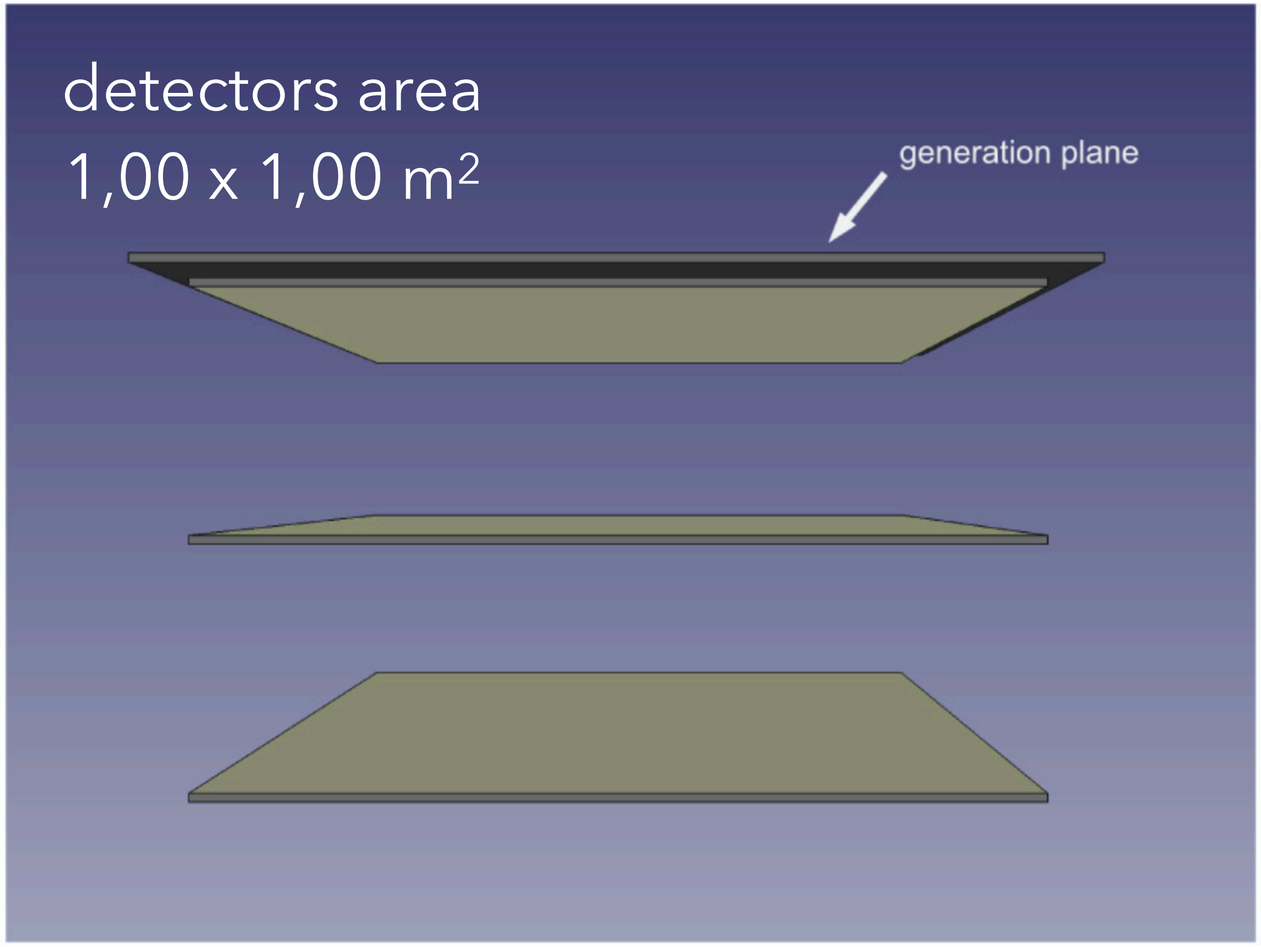

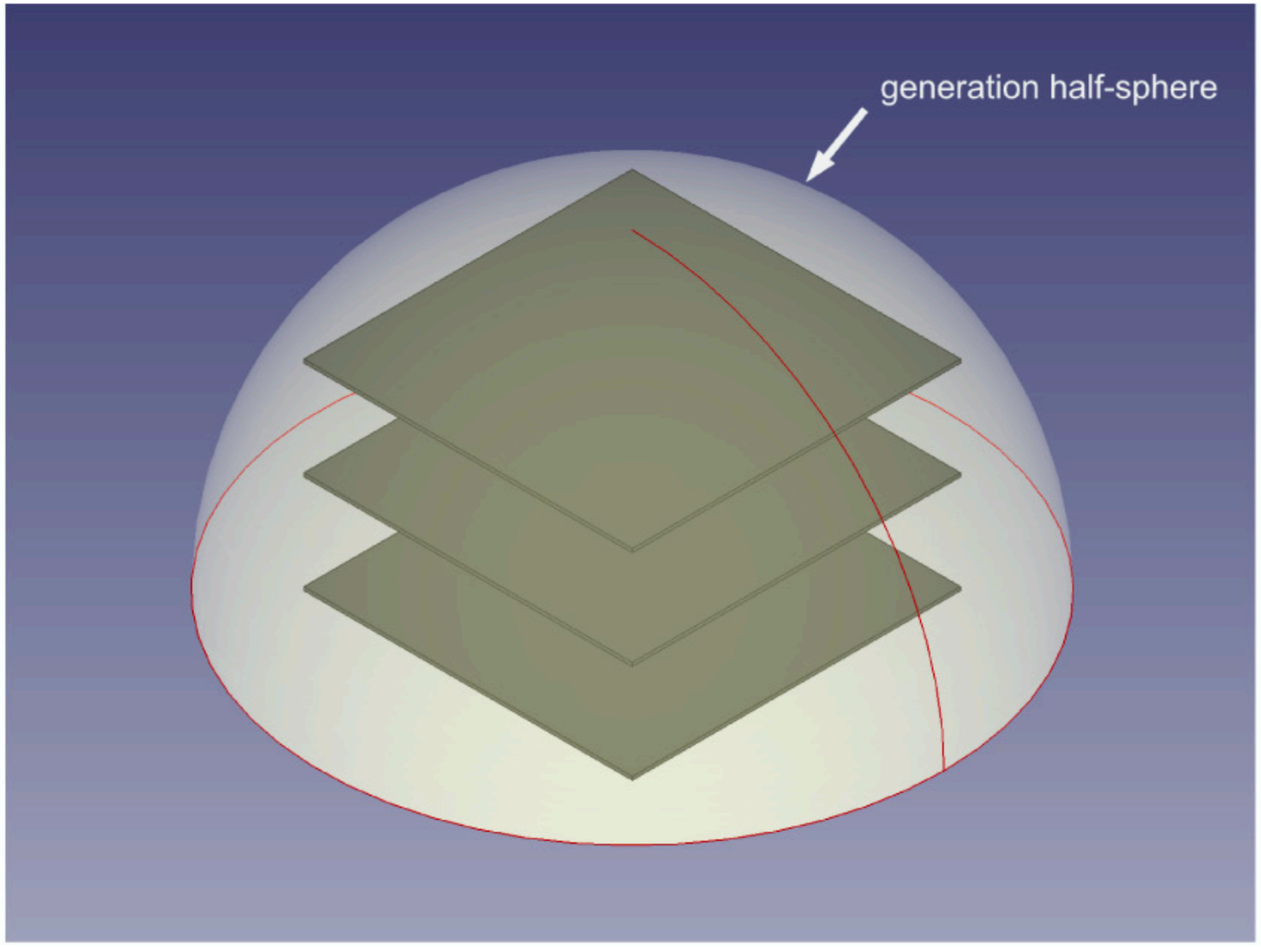

Example 3: a vertex detector

- we generate over a flat sky, a cylindrical and a half-spherical surface
- we require the muon to cross two elements of an octagonal detector
- we compare the distributions of p, θ and Φ (filtered by two elements)

Modes comparison - EcoMug

4. Comparison between the different generation methods

The generation methods discussed above, and implemented in Eco-Mug, are mathematically equivalent, provided that all of them grant the proper coverage of the geometrical acceptance of the detection system. However, depending on the case study, one method could be more effective than the others, in respect to the generation time. In this section, a comparison of the performance of the three generation methods, for three different scenarios, is presented.

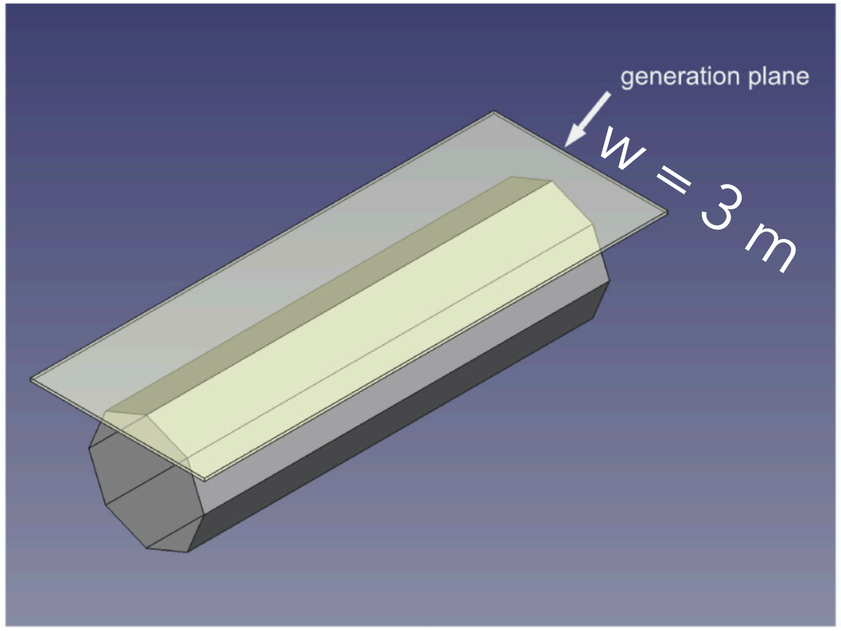

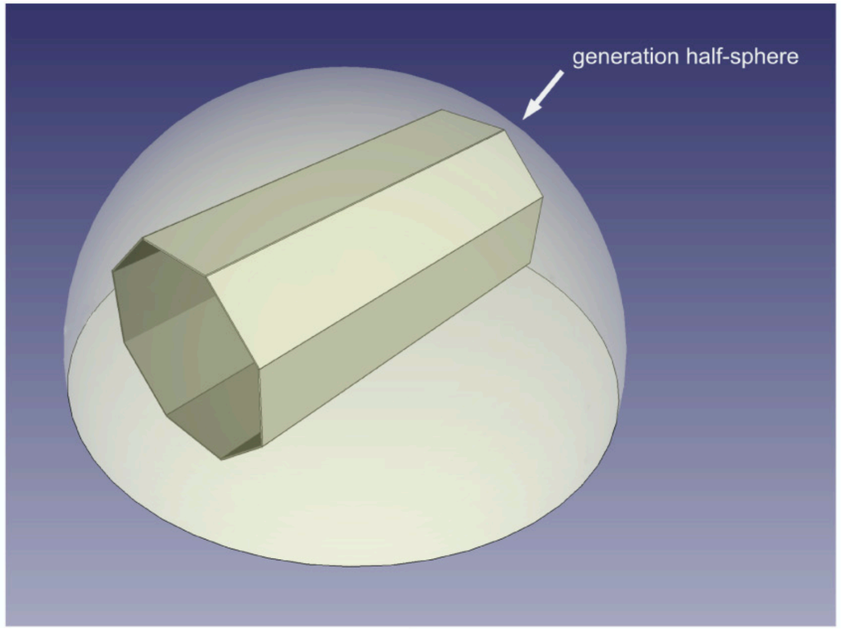

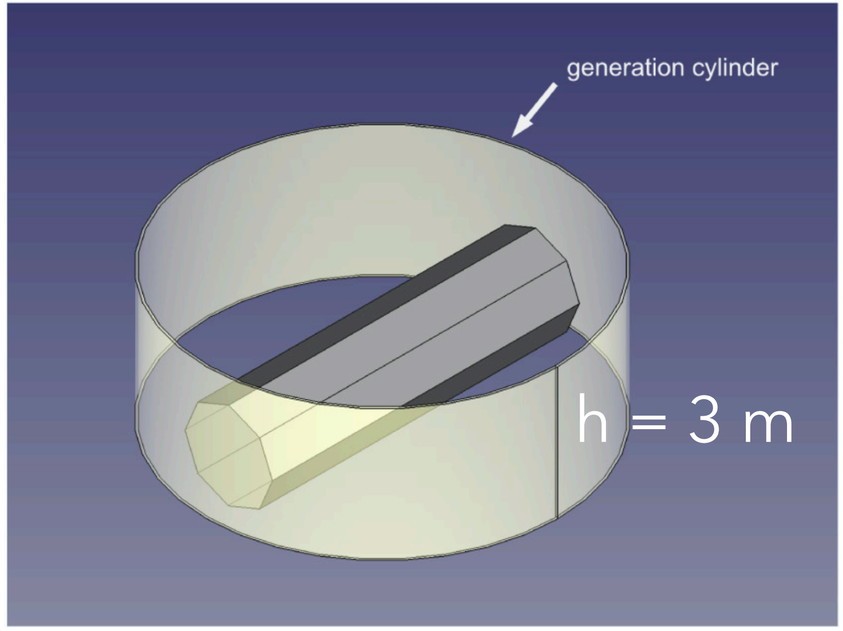

Limitations

Limited to surface parameterizations

o) EcoMug generates muons from parameterizations of experimental surface fluxes, so it does not simulate the full atmospheric cascade → No direct modeling of primary cosmic rays or shower development

Flux parameters from a single measurement

o) Not automatically tunable for different conditions (**no altitude, pressure and temperature, latitude, underground, underwater handles**). On the other hand, it can be tuned manually knowing the desired differential flux behavior.

o) Experimental data measured the differential flux of the charged component in cosmic rays: at lower momenta and large values of θ the contribution due to **electrons** is relevant (they are not taken into account). Because of this, measured flux starts to increase quickly as the momentum decreases. Chosen parametrization, however, does not include this effect, as only the muon component is relevant to EcoMug, resulting in a discrepancy for low momenta and large zenith angles.

o) For many applications in muon radiography and tomography, high energy and nearly horizontal cosmic- ray muons are of utmost importance. By default EcoMug generates them with momentum up to **1000 GeV/c and zenith angles up to 90º**. The user should keep in mind, though, that EcoMug could not describe accurately the flux outside the range of experimental data (**up to approximately 100 GeV/c and up to 80º**)

Appendix. Example of integration with GEANT4

EcoMug can be easily integrated with GEANT4, by modifying the (mandatory) user action class derived from `G4VUserPrimaryGeneratorAction`.

The relevant lines of codes to be included in the header file are reported below.

```
#include "EcoMug.h"
...
class PrimaryGeneratorAction :
      public G4VUserPrimaryGeneratorAction {
  public:
  ...
  G4ParticleGun *fParticleGun;
  G4ParticleDefinition *mu_plus, *mu_minus;
  EcoMug fMuonGen;
};
```

The implementation file initializes the class `EcoMug` and interfaces it to `G4ParticleGun`, as shown in the code below.

```
PrimaryGeneratorAction::PrimaryGeneratorAction() :
G4VUserPrimaryGeneratorAction(),
fParticleGun(0), mu_plus(0), mu_minus(0) {
  fMuonGen.SetUseCylinder();
  fMuonGen.SetCylinderRadius(2500*mm);
  fMuonGen.SetCylinderHeight(4170*mm);

  fParticleGun  = new G4ParticleGun(1);
  mu_minus  = G4ParticleTable::GetParticleTable()
              ->FindParticle("mu-");
  mu_plus  = G4ParticleTable::GetParticleTable()
             ->FindParticle("mu+");
}
...
void PrimaryGeneratorAction::GeneratePrimaries(G4Event* ev) {
  fMuonGen.Generate();
  array<double, 3> muon_pos = fMuonGen.GetGenerationPosition();
  double muon_ptot = fMuonGen.GetGenerationMomentum();
  double muon_theta = fMuonGen.GetGenerationTheta();
  double muon_phi = fMuonGen.GetGenerationPhi();
  fParticleGun->SetParticlePosition(G4ThreeVector(
    muon_pos[0]*mm,
    muon_pos[1]*mm,
    muon_pos[2]*mm
  ));

  fParticleGun->SetParticleMomentum(G4ParticleMomentum(
    muon_ptot*sin(muon_theta)*cos(muon_phi)*GeV,
    muon_ptot*sin(muon_theta)*sin(muon_phi)*GeV,
    muon_ptot*cos(muon_theta)*GeV
  ));

  // charge
  if (fMuonGen.GetCharge() < 0) {
    fParticleGun->SetParticleDefinition(mu_minus);
  } else {
    fParticleGun->SetParticleDefinition(mu_plus);
  }
  fParticleGun->GeneratePrimaryVertex(ev);
}
```

5.1. Basic usage

The use of the library requires the initialization of the EcoMug class, the choice of the generation method, and the definition of the size and position of the generation surface, as in the example codes 1, 2 and 3.

```
EcoMug gen; // initialization of the class
gen.SetUseSky(); // plane surface generation
gen.SetSkySize({{10., 10.}}); // x and y size of the plane
// (x,y,z) position of the center of the plane
gen.SetSkyCenterPosition({{0., 0., 20.}});
```

Example code 1: EcoMug setup for a flat surface generation.

```
EcoMug gen; // initialization of the class
gen.SetUseCylinder(); // cylindrical surface generation
gen.SetCylinderRadius(10.); // cylinder radius
gen.SetCylinderHeight(30.); // cylinder height
// (x,y,z) position of the center of the cylinder
gen.SetCylinderCenterPosition({{0., 0., 15.}});
```

Example code 2: EcoMug setup for a cylindrical surface generation.

```
EcoMug gen; // initialization of the class
gen.SetUseHSphere(); // half-spherical surface generation
gen.SetHSphereRadius(30.); // half-sphere radius
// (x,y,z) position of the center of the half-sphere
gen.SetHSphereCenterPosition({{0., 0., 0.}});
```

Example code 3: EcoMug setup for a half-spherical surface generation.

```
// Setup of the instance of the EcoMug class
// as in the example code 1
EcoMug gen;
gen.SetUseSky();
gen.SetSkySize({{10., 10.}});
gen.SetSkyCenterPosition({{0., 0., 20.}});

// The array storing muon generation position
std::array<double, 3> muon_position;

// Loop to generate 1000 cosmic-ray muons
for (auto event = 0; event < 1000; ++event) {
  gen.Generate(); // generate a cosmic-ray muons

  // access position, direction and momentum
  // pleas note that GetGenerationPosition()
  // returns a std::array<double, 3>
  muon_position = gen.GetGenerationPosition();
  double muon_p = gen.GetGenerationMomentum();
  double muon_theta = gen.GetGenerationTheta();
  double muon_phi = gen.GetGenerationPhi();
  double muon_charge = gen.GetCharge();

  ... // the code where generated CR muons are used
}
```

Example code 4: Accessing position, direction, momentum and charge of generated cosmicray muons in EcoMug.

In several scenarios, one could be interested in generating tracks from a subset of these parameters, saving space and computation time. EcoMug allows this by exposing to the user the following methods:

- `SetMinimumMomentum` - Set the minimum momentum for generated cosmic-ray muons;
- `SetMaximumMomentum` - Set the maximum momentum for generated cosmic-ray muons;
- `SetMinimumTheta` - Set the minimum zenith angle θ for generated cosmic-ray muons;
- `SetMaximumTheta` - Set the maximum zenith angle θ for generated cosmic-ray muons;
- `SetMinimumPhi` - Set the minimum azimuthal angle ϕ for generated cosmic-ray muons;
- `SetMaximumPhi` - Set the maximum azimuthal angle ϕ for generated cosmic-ray muons.

The full list of methods of the EcoMug class is available at the following link:
https://dr4kan.github.io/EcoMug/class_eco_mug.html.

5.4. *Using a user-defined function for the differential flux*

In those cases where the proposed parametrization of J does not provide an accurate description of the differential flux of CR muons, EcoMug gives the possibility to use a custom function for J, as shown in the example code 7.

```
double J(double p, double theta) {
  double A = 0.14*pow(p, -2.7);
  double B = 1. / (1. + 1.1*p*cos(theta)/115.);
  double C = 0.054 / (1. + 1.1*p*cos(theta)/850.);
  return A*(B+C);
}

EcoMug gen;
gen.SetUseSky();
gen.SetSkySize({{x, y}});
gen.SetSkyCenterPosition({0., 0., z});
gen.SetMinimumMomentum(150);
gen.SetDifferentialFlux(&J);

for (auto event = 0; event < nevents; ++event) {
  gen.GenerateFromCustomJ(); // generate from user-defined J
  ... // retrieve and use muon data
  gen.Generate(); // generate from J as in equation 2
  ... // retrieve and use muon data
}
```

Example code 7: Filtering the generation in EcoMug.

In the previous code, the same instance of the class `EcoMug` is used to generate according to a Gaisser-like parametrization [41] and to the default one (Eq. (2)). The use of a custom definition for J requires a function of both momentum and θ to be passed to the generator by means of the method `SetDifferentialFlux`. Afterwards, the user can invoke the generation of a CR muon, according to the specified J, with the method `GenerateFromCustomJ`.

An example of VMC

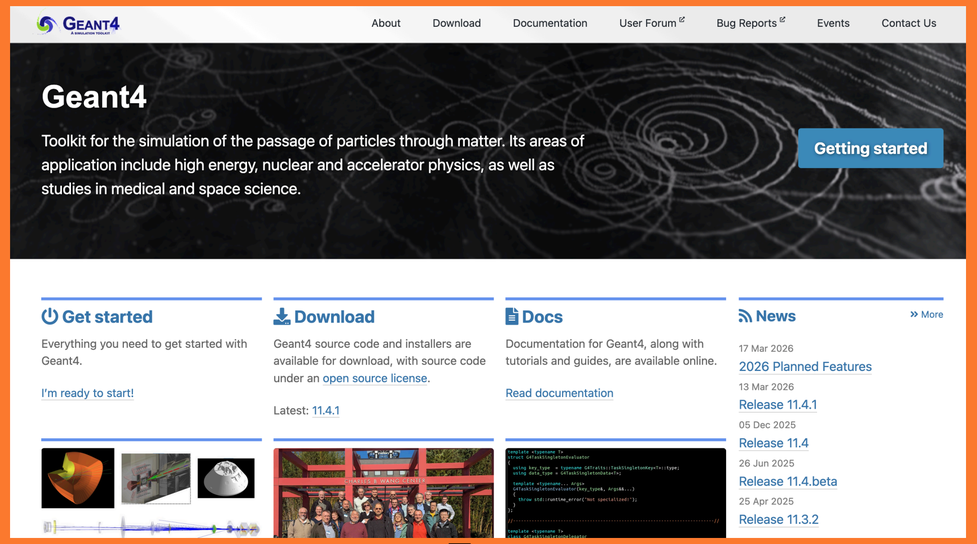

+

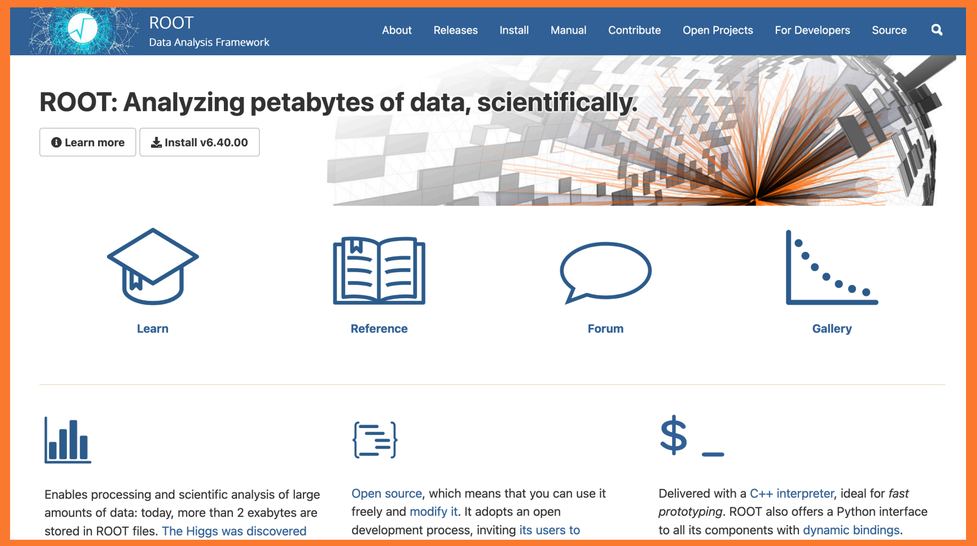

=

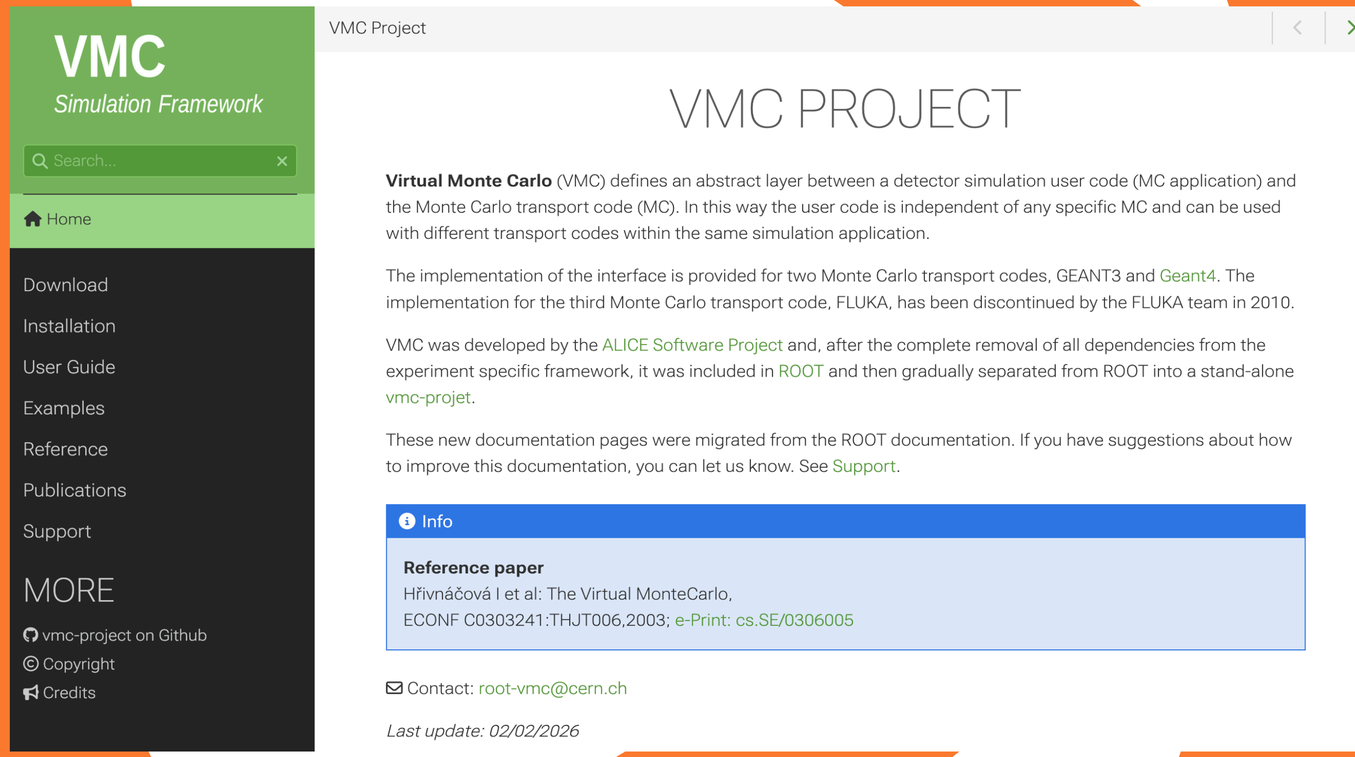

https://vmc-project.github.io/

uReactor project

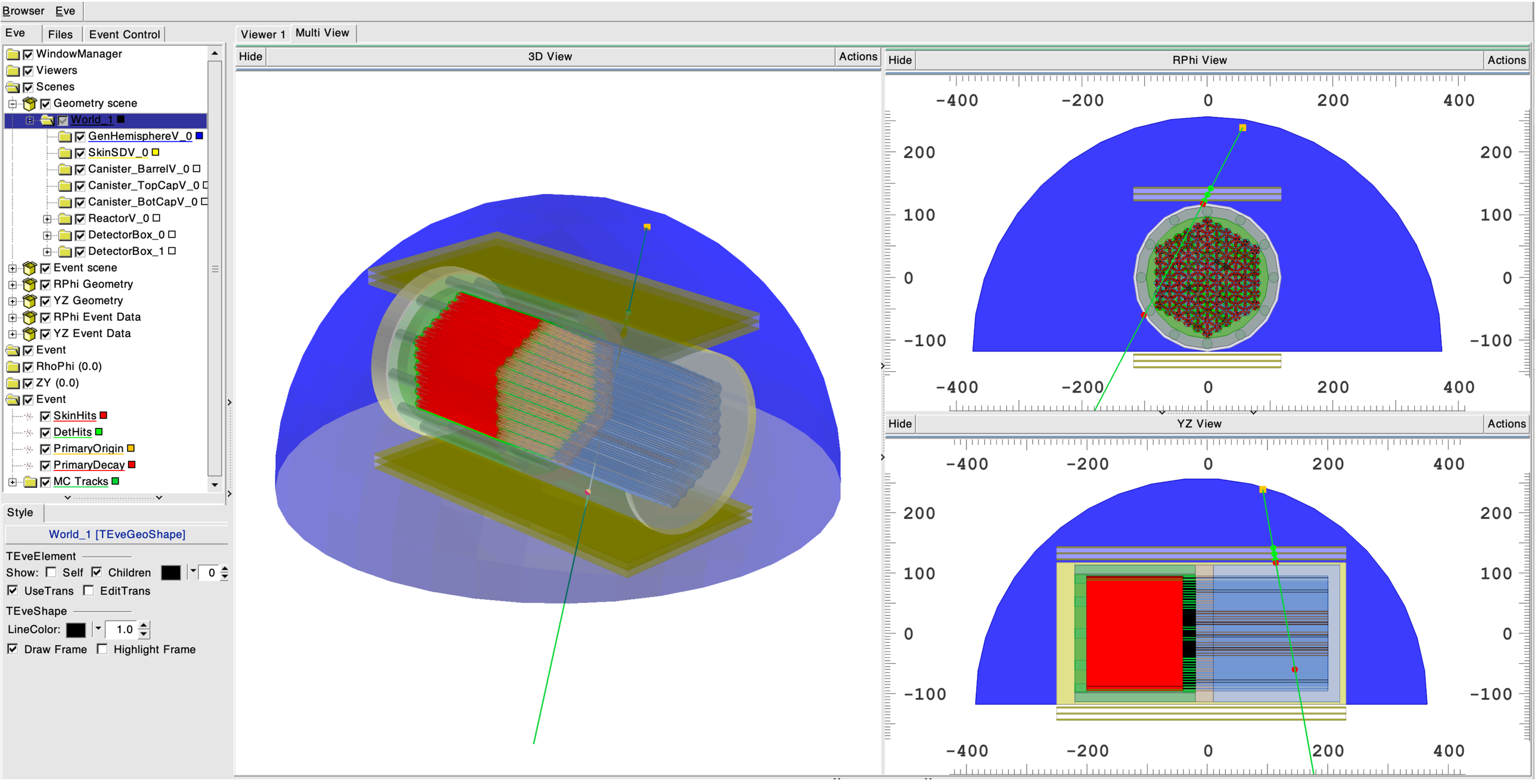
Browser
Eve
Eve
Files
Event Control
WindowManager
Viewers
Scenes
Geometry scene
World_1
GenHemisphereV_0
SkinSDV_0
Canister_BarrelV_0
Canister_TopCapV_0
Canister_BotCapV_0
ReactorV_0
DetectorBox_0
DetectorBox_1
Event scene
RPhi Geometry
YZ Geometry
RPhi Event Data
YZ Event Data
Event
RhoPhi (0.0)
ZY (0.0)
Event
SkinHits
DetHits
PrimaryOrigin
PrimaryDecay
MC Tracks
Style
World_1 [TEveGeoShape]
TEveElement
Show: Self Children 0
UseTrans EditTrans
TEveShape
LineColor: 1.0
Draw Frame Highlight Frame
Viewer 1
Multi View
Hide
3D View
Actions
Hide
RPhi View
Actions
-400
-200
0
200
400
200
100
0
-100
Hide
YZ View
Actions

Backup

CORSIKA (D. Heck, T. Pierog, J. Knapp, CORSIKA: An air shower simulation program, Astrophys. Source Code Libr. (2012) ascl–1202)

The most popular CRAS generator, specifically tailored to the simulation of air showers initiated by primary cosmic rays, is CORSIKA

CORSIKA (COsmic Ray SImulation for KAscade) is a Monte Carlo toolkit to simulate the evolution of EAS in the atmosphere initiated by photons, protons, nuclei or any other particle. All particles are tracked through the atmosphere until they either interact, decay or are absorbed.

AIRES (10.48550/arXiv.astro-ph/9911331)
AIRES is a Monte Carlo simulation program designed to model
the development of extensive air showers (EAS) produced by high-energy cosmic rays interacting with the Earth’s atmosphere.

CRY (http://dx.doi.org/10.1109/nssmic.2007.4437209)

CRY generates all produced particles (not only muons), which is why it has been included in the CRAS generators category, but at a fraction of the time required by CORSIKA. The user can choose to generate particle shower distributions at three different elevations (sea level, 2100 m and 11300 m) and has control over the geomagnetic cutoff and solar cycle effects. The gain in performance over CORSIKA comes at a cost: only protons are used for cosmic primaries, the energy range is limited, and the atmospheric modeling is simplified

FLUKA

FLUKA is a general-purpose Monte Carlo transport and interaction code used for fundamental physics and a wide range of applications, including cosmic ray physics (muons, neutrinos, EAS, underground physics). It covers the simulation of the formation and propagation of electromagnetic and hadronic showers in the Earth's atmosphere.

MuTEV (http://dx.doi.org/10.1016/j.nima.2010.05.019**)**

muTeV is a FLUKA-based generator for TeV muons, mainly dedicated to the physics of high energy muons in underground or underwater experiments. The code, together with FLUKA, takes care of the interaction of primary cosmic ray in the atmosphere, modeled as a set concentric spherical shells, the air shower development, the transportation through the overburden (rock or sea), and the muon detection simulation. 3D profiles of the Gran Sasso mountain, as well as of the sea above two locations of underwater experiments, are already encoded in the software and new ones can be defined by the user.

MUPAGE (http://dx.doi.org/10.1016/j.cpc.2008.07.014**)**

MUPAGE has been developed to generate single and multiple atmospheric muon events, mainly for underwater/ice neutrino telescopes. MUPAGE relies on parametric formulas describing flux, angular distribution and energy of muon bundles, for water equivalent (w.e.) depths between 1.5 km to 5 km and zenith angles between 0 and 85○. The parametrization was obtained by means of MC simulations of primary cosmic ray interactions and shower propagation in the atmosphere, using the HEMAS code [34]. The choice of HEMAS (instead of the much more popular CORSIKA) was due to the fact that it was previously cross-checked with data from the underground MACRO experiment, operating from 1994 to 2000 at the Gran Sasso laboratories, at a w.e. depth comparable to that of neutrino telescopes

Differential flux

Number of cosmic-ray muons in a interval of time dt,

with momentum between p and p+dp,

with zenith angle between θ and θ + dθ,

with azimuthal angle between Φ and Φ + dΦ,

crossing a surface ***dS_n perpendicular to the muon direction***

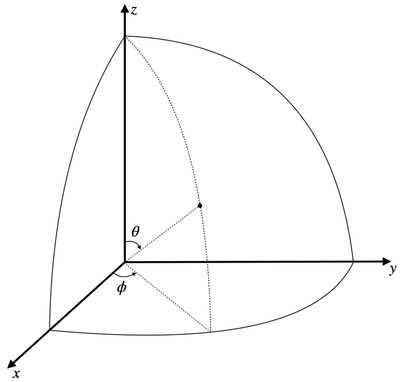

$$J'(t,p,\theta,\phi) = \frac{dN}{dt \cdot dp \cdot d\theta \cdot d\phi \cdot dS_n}$$

… crossing a ***horizontal surface dS_z***

$$J'_z(t,p,\theta,\phi) = \frac{dN}{dt \cdot dp \cdot d\theta \cdot d\phi \cdot dS_z}$$

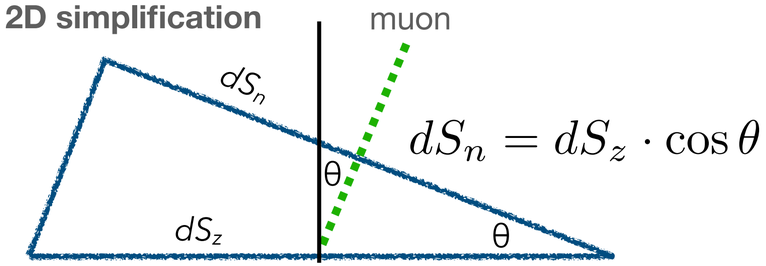

$$dS_n = dS_z \cdot \cos\theta$$

$$J'_z(t,p,\theta,\phi) = J'(t,p,\theta,\phi) \cdot \cos\,\theta$$

$$J'_z \equiv \frac{dN}{dt \cdot dp \cdot d\theta \cdot d\phi \cdot dS_z} = \left[1600 \cdot \left(\frac{p}{p_0} + 2.68\right)^{-3.175} \cdot \left(\frac{p}{p_0}\right)^{0.279}\right] \cdot (\cos\theta)^{n+1} \cdot \sin\theta \cdot \frac{1}{\mathrm{m}^2 \cdot \mathrm{s} \cdot \mathrm{sr} \cdot \mathrm{GeV/c}}$$

Differential flux

Number of cosmic-ray muons in a interval of time dt,

with momentum between p and p+dp,

with zenith angle between θ and θ + dθ,

with azimuthal angle between Φ and Φ + dΦ,

crossing a surface ***dS_n perpendicular to the muon direction***

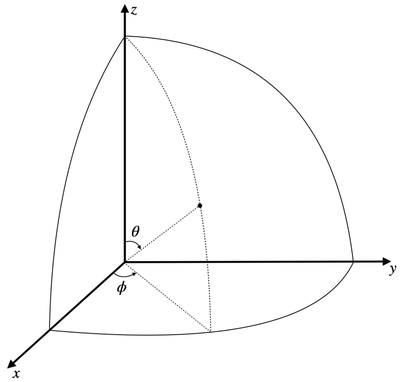

$$J'(t,p,\theta,\phi) = \frac{dN}{dt \cdot dp \cdot d\theta \cdot d\phi \cdot dS_n}$$

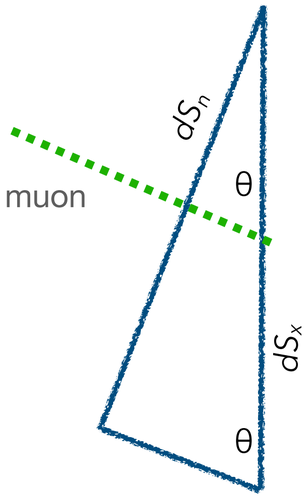

2D simplification

$$dS_n = dS_x \ \hat{x} \cdot \hat{n} = dS_x \sin\theta \cos\phi$$

Cylindrical symmetry => vertical surface dS_x
Cylinder lateral surface => also Φ plays a role

$$J'_x(t,p,\theta,\phi) = \frac{dN}{dt \cdot dp \cdot d\theta \cdot d\phi \cdot dS_x}$$

… crossing a ***vertical surface dS_x***

$$J'_x(t,p,\theta,\phi) = J'(t,p,\theta,\phi) \cdot \sin\theta \cdot \cos\phi$$

$$J'_x \equiv \frac{dN}{dt \cdot dp \cdot d\theta \cdot d\phi \cdot dS_x} = \left[1600 \cdot \left(\frac{p}{p_0} + 2.68\right)^{-3.175} \cdot \left(\frac{p}{p_0}\right)^{0.279}\right] \cdot (\cos\theta)^n (\sin\theta)^2 \cos\phi \cdot \frac{1}{\mathrm{m}^2 \cdot \mathrm{s} \cdot \mathrm{sr} \cdot \mathrm{GeV/c}}$$

Differential flux

Number of cosmic-ray muons in a interval of time dt,

with momentum between p and p+dp,

with zenith angle between θ and θ + dθ,

with azimuthal angle between Φ and Φ + dΦ,

crossing a surface ***dS_n perpendicular to the muon direction***

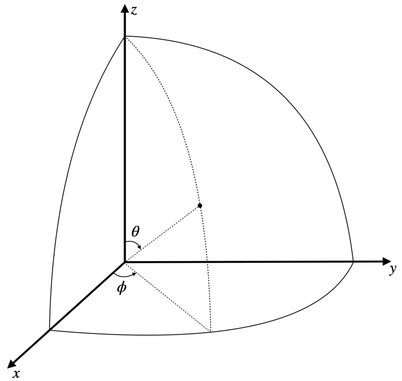

$$J'(t,p,\theta,\phi) = \frac{dN}{dt \cdot dp \cdot d\theta \cdot d\phi \cdot dS_n}$$

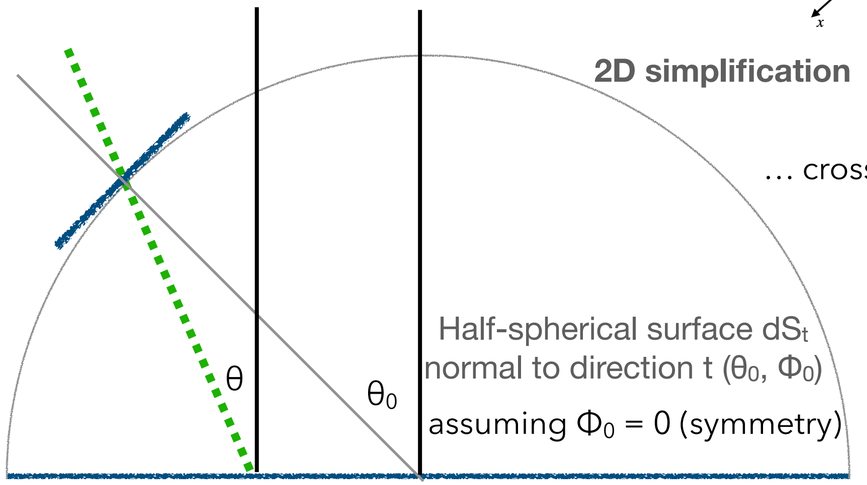

… crossing a ***surface dS_t (θ_0, Φ_0)***

$$J'_t(t,p,\theta,\phi) = \frac{dN}{dt \cdot dp \cdot d\theta \cdot d\phi \cdot dS_t}$$

$$J'_t(t,p,\theta,\phi) = J'(t,p,\theta,\phi) \cdot [\sin\theta_0 \sin\theta \cos\phi + \cos\theta_0 \cos\theta]$$

$$dS_n = dS_t \; \hat{t} \cdot \hat{n} = dS_t \, [\sin\theta_0 \sin\theta \cos\phi + \cos\theta_0 \cos\theta]$$

$$J'_t \equiv \frac{dN}{dt \cdot dp \cdot d\theta \cdot d\phi \cdot dS_t} = \left[1600 \cdot \left(\frac{p}{p_0} + 2.68\right)^{-3.175} \cdot \left(\frac{p}{p_0}\right)^{0.279}\right] \cdot (\cos\theta)^n \left[\sin\theta_0 (\sin\theta)^2 \cos\phi + \cos\theta_0 \cos\theta \sin\theta\right] \cdot \frac{1}{\mathrm{m}^2 \cdot \mathrm{s} \cdot \mathrm{sr} \cdot \mathrm{GeV/c}}$$